

Multiple-scattering model for the coherent reflection and transmission of light from a disordered monolayer of particles

Augusto García-Valenzuela,^{1,*} Edahí Gutiérrez-Reyes,² and Rubén G. Barrera²

¹*Departamento de Física, Universidad Autónoma Metropolitana Iztapalapa, Apartado Postal 55-534, Distrito Federal 09340, México*

²*Instituto de Física, Universidad Nacional Autónoma de México, Apartado Postal 20-364, Distrito Federal 01000, México*

*Corresponding author: augusto.garcia@ccadet.unam.mx

Received September 15, 2011; revised January 20, 2012; accepted January 20, 2012;
posted January 23, 2012 (Doc. ID 154647); published June 1, 2012

Using a multiple-scattering formalism, we derive closed-form expressions for the coherent reflection and transmission coefficients of monochromatic electromagnetic plane waves incident upon a two-dimensional array of randomly located spherical particles. The calculation is performed within the quasi-crystalline approximation, and the statistical correlation among the particles is assumed to be given simply by a correlation hole. In the resulting model, the size of the spheres and the angle of incidence are both unrestricted. The final formulas are relatively simple, making the model suitable for a straightforward interpretation of optical-sensing measurements. © 2012 Optical Society of America

OCIS codes: 290.5850, 290.4210, 240.0240, 290.7050.

1. INTRODUCTION

The optical properties of monolayers of small particles are of interest, for instance, in the design of diverse physical and chemical sensors consisting of a monolayer of metallic particles interacting with their environment, and where changes of their physical or chemical state are detected through changes of their optical reflectivity (e.g., see [1–4]).

In practice, the particles of a monolayer are usually supported and randomly located over a flat substrate. When the particles in a monolayer are very small compared to the wavelength of an incident beam, the beam will be reflected only specularly. However, when particles are not that small, the beam will be reflected partly specularly, but it will be also scattered in all different directions. Furthermore, if the size of the particles is comparable to or larger than the wavelength of the incident radiation, almost all light will be scattered. But besides their size, the contrast in their index of refraction relative to the one of the environment also becomes a relevant factor for their scattering power: the larger the contrast, the larger the scattering.

It is found convenient to split the fields reflected and transmitted by the monolayer into two components: a coherent component and a diffuse one. The coherent component travels in only one direction and its amplitude is independent on the specific random location of the particles, while the diffuse component travels in many directions with amplitudes that do depend on the specific location of the particles. Therefore if one takes an ensemble average over the random location of the particles, only the coherent component will survive, and for this reason the coherent component is also called the average field, while the diffuse component is known also as the fluctuation field, meaning with this, that it is the field left after the average field is subtracted from the total

field. Being the power a quadratic quantity in the fields that travels in the direction of the Poynting vector, the ensemble average of the power carried by the reflected and transmitted fields has two components, one coming from the average of the product of the amplitudes of the coherent field and traveling in only one direction, plus another one coming from the average of the product of the amplitudes of the fluctuating field and traveling in many different directions. The cross product of the coherent and fluctuating amplitudes averages to zero. We define the coherent reflectance and the coherent transmittance of a random monolayer as the ratio between the average power carried only by the coherent component of the reflected or transmitted fields and the incident power. The coherent reflectance actually corresponds to what authors usually refer as reflectivity and it is the one that will be considered in this work. The relative amount of average power carried by the coherent and the diffuse components depends on the angle of incidence as well as on the size and refractive index of the particles. In experiments it is relatively simple to separate the average power carried by the coherent component from the one carried by the diffuse one in the the specular direction, this is done by performing power measurements as a function of the angle and interpolating the measurements of the diffuse component across the specular direction.

The problem of reflection and transmission of light by a monolayer of very small particles, either supported by a flat interface or embedded in a transparent medium, has received extensive attention over the years [5–17]. In most of these works an effective-medium approach has been developed and used. If the particles are small, but not sufficiently small, the effective-medium approach requires an extension [10–12]. But when the size of the particles is comparable to or larger

than the wavelength of the incident radiation the rewards from effective-medium theories are lost in many respects and a multiple-scattering approach is required [18,19,20]. A fairly complete presentation of the multiple-scattering approach for electromagnetic wave propagation through random systems of discrete scatterers can be found in [21].

The multiple-scattering approach has been used by a few authors, at different levels of approximation, in the problem of coherent reflection and transmission of light from a monolayer of particles supported on a flat surface [22–29]. Up to date, either the single-scattering approximation (SS) or numerical solutions to the so called quasi-crystalline approximation (QCA) in the hierarchy of multiple-scattering equations, has been used. Numerical solutions within the QCA [24,26,28,30] require a good deal of computational effort and, as most numerical schemes, they offer little physical insight into the problem. A relatively simple heuristic model (HM) that goes beyond the SS while keeping a comparable simplicity was recently put forth by our group [29]. This HM behaves well for all angles of incidence and particle sizes. It is, however, limited to a small surface coverage of the monolayer. The results of this model were found to be consistent with experimental data of reflectivity measurements in an internal reflection configuration from a sparse monolayer of large particles adsorbed at the base of a glass prism [29]. The simplicity of the expressions for the reflection and transmission coefficients for the coherent wave of the HM makes it very attractive for the straightforward analysis of new problems in practical applications. However, its heuristic nature prevents a deeper analysis of the model and its limitations, undermining the confidence of its use.

Therefore our present objective in this paper is to derive closed-form expressions for the reflectivity and transmissivity coefficients of a random monolayer of particles and with similar simplicity to the heuristic model in [29], but derived from a multiple-scattering theory with well-identifiable approximations.

In this paper we start by reviewing some basic concepts and setting, within the QCA, an integral equation for the average electric field exciting the particles in a monolayer illuminated by an external plane monochromatic wave. We obtain an approximate solution to this equation using a simple correlation-hole model for the two-particle correlation function and assuming an Ansatz for the exciting field consisting of two effective traveling plane monochromatic waves. We show that, to a good approximation our Ansatz solves the QCA equation when the surface-coverage-fraction is moderately small. In this way we obtain analytical expressions for the coherent reflection and transmission coefficients which behave well at any angle of incidence and particle size. These results, while retaining comparable simplicity, reduce to the HM and the SS previously mentioned for sufficiently small coverage fraction. The model so obtained can be readily used in many applications relating optical phenomena with disordered monolayers of particles.

In Section 2 we review the multiple-scattering formalism and the QCA. In Section 3 we find approximate solutions to the QCA integral equation for a free-standing monolayer of particles and in Section 4 we provide formulas to take into account the presence of the substrate supporting the particles. In Section 5 we present a few numerical examples of the

predictions of the formulas for the coherent reflectance and transmittance of free-standing and supported monolayers. Finally in Section 6 a couple of remarks about the behavior of our model for grazing incidence and in the limit of small particles are made and in Section 7 we present a summary and our conclusions.

2. MULTIPLE-SCATTERING FORMALISM

Let us first assume a system of N identical particles randomly positioned within a volume V in space. Let us assume the particles are embedded in a homogeneous, nonmagnetic medium of refractive index n_m . We will refer to this medium surrounding the particles as the matrix. For simplicity let us suppose all particles are spherical and have the same radius a and refractive index n_p . We will indicate the position of the particles in space by the coordinates of their centers, \mathbf{r}_n , with $n = 1, 2, \dots, N$. In a monolayer of identical particles, the centers of all particles lie on a plane as illustrated in Fig. 1. However, let us assume here the more general case of a random system of particles whose centers are enclosed in a thin film of volume V . The monolayer case is later obtained by letting the thickness of the film become arbitrarily thin.

Let us suppose the plane wave $\mathbf{E}^i(\mathbf{r}, t) = E_0 \exp(i\mathbf{k}^i \cdot \mathbf{r} - i\omega t)\hat{\mathbf{e}}_i$ is incident to the system of particles, where $\mathbf{k}^i = k_y^i \hat{\mathbf{a}}_y + k_z^i \hat{\mathbf{a}}_z$ with $k_y^i = k_m \sin \theta_i$, $k_z^i = k_m \cos \theta_i$, $k_m = 2\pi n_m / \lambda$, and λ is the wavelength of light in vacuum. Here $\hat{\mathbf{a}}_x$, $\hat{\mathbf{a}}_y$, and $\hat{\mathbf{a}}_z$ denote unit vectors along the x , y , and z Cartesian axes, respectively. The incident electric field, oscillating at a frequency ω , induces currents in each particle and these currents produce a field that we will call the induced field. Since we assume the particles have a linear response to an electromagnetic excitation at the frequency of the incident light, the induced electric field produced by the n th particle oscillates also at a frequency ω and its amplitude can be written as

$$\mathbf{E}_n^{\text{ind}}(\mathbf{r}; \omega) = i\omega\mu_0 \int \overleftrightarrow{\mathbf{G}}(\mathbf{r}, \mathbf{r}'; \omega) \cdot \mathbf{J}_{\text{ind}}^{(n)}(\mathbf{r}'; \omega) d^3r', \quad (1a)$$

where the integral is over all space, μ_0 is the magnetic permeability of vacuum, and $\mathbf{J}_{\text{ind}}^{(n)}(\mathbf{r}'; \omega)$ is the total current density induced within the particles which is in excess of the current that would have been induced in the matrix (the background medium) without the particle. $\mathbf{J}_{\text{ind}}^{(n)}(\mathbf{r}'; \omega)$ includes all excess currents, whether they are polarization, conduction, or magnetization currents. The total induced field is the sum of the fields produced by the currents induced in all particles. Here $\overleftrightarrow{\mathbf{G}}(\mathbf{r}, \mathbf{r}'; \omega)$ is the dyadic Green's function of the vector wave equation in the background medium which obeys

$$(\nabla \times \nabla \times - k_M^2) \overleftrightarrow{\mathbf{G}}(\mathbf{r}, \mathbf{r}'; \omega) = \overleftrightarrow{\mathbf{1}} \delta(\mathbf{r} - \mathbf{r}'), \quad (1b)$$

where $k_M \equiv 2\pi/\lambda_M$ and λ_M is the wavelength of the free-propagating waves in the matrix oscillating with frequency ω . As in Eq. (1a), when the limits of an integral are not indicated it is meant that the integral is over all the space available to the integration variable, otherwise, the limits of the integrals will be indicated.

Let us recall that $\overleftrightarrow{\mathbf{G}}$ is singular at $\mathbf{r} = \mathbf{r}'$ and it is therefore undefined in the sense of a classical function and one has to be cautious when performing the integration in Eq. (1a) in the source region. Besides, the presence of the delta function in

Eq. (1b) prescribes that $\vec{\mathbf{G}}$ should be considered as a distribution or generalized function, which implies that only the integral over $\vec{\mathbf{G}}$ times a wide class of test functions makes sense. Nevertheless there is also a standard procedure for taking care of the singularities in the source region in Eq. (1a): the principal volume integration, in which the singular points are surrounded by either an infinitesimal or a finite small volume of a definite shape, whose contributions to the integral are evaluated separately. It has been shown that, at least for the dyadic Green's function in free space, this procedure yields the correct result (see for example [31]), being also the one used in this work.

Here, our definition of induced fields includes the fields inside and outside the particles. We can separate the field induced by one given particle in the field scattered by that particle, defined only outside the particle, and the induced internal-field, defined only inside the particle. The induced internal-field in a particle is given by the total internal-field minus the external field exciting that particle.

The current induced in a particle centered at \mathbf{r}_n can be related to the exciting field, that is, the external field plus the field scattered by all other particles but the n th one, through a linear relation known as nonlocal Ohm's law, and given by

$$\mathbf{J}_{\text{ind}}^{(n)}(\mathbf{r}') = \int d^3r'' \vec{\sigma}(\mathbf{r}' - \mathbf{r}_n, \mathbf{r}'' - \mathbf{r}_n) \cdot \mathbf{E}_n^{\text{exc}}(\mathbf{r}''), \quad (2a)$$

where $\vec{\sigma}$ is defined through Eq. (2a) and is called generalized nonlocal conductivity [20]. For brevity in the notation we have suppressed the argument ω and we will continue to do that unless it leads to confusion. It has been also shown that $\vec{\sigma} = (1/i\omega\mu_0)\mathbf{T}$, where \mathbf{T} is the transition operator (T matrix) used in scattering theory [20]. This relation serves to connect the effective-medium approach centered in the calculation of an effective conductivity with the multiple-scattering approach. Let us recall that \mathbf{T} obeys a Lippmann–Schwinger integral equation, which in our case can be written as [20,32]

$$\vec{\mathbf{T}}(\mathbf{r}, \mathbf{r}') = U(\mathbf{r}) \left[\delta(\mathbf{r} - \mathbf{r}') \vec{\mathbf{I}} + \int_{V_S} d^3r'' \vec{\mathbf{G}}(\mathbf{r}, \mathbf{r}'') \cdot \vec{\mathbf{T}}(\mathbf{r}'', \mathbf{r}') \right], \quad (2b)$$

where V_S is the volume of the spheres and $U(\mathbf{r}) = 0$ for $\mathbf{r} \notin V_S$ and $U(\mathbf{r}) = i\omega\mu_0(\sigma_S - \sigma_M)$ for $\mathbf{r} \in V_S$. Here σ_S and σ_M are the local complex conductivities of the spheres and of the matrix, respectively. Since we assume that, in the frequency range of interest the matrix is nondissipative, $\sigma_M = -i\omega(\epsilon_M - \epsilon_0)$ will be purely imaginary, that is, the dielectric function ϵ_M of the matrix will be real. We are using SI units. Although one rarely has an explicit expression for the transition operator, in this work we will only use a few of its projections in Fourier space which can be related to the elements of the amplitude scattering matrix of an isolated particle (see for instance [18]–[21]). These, in turn, are readily calculated for spherical particles using Mie theory (see for example [32]). The total electric field defined as the incident field plus the field induced in the system of N particles, can be written as

$$\mathbf{E}(\mathbf{r}) = \mathbf{E}^i(\mathbf{r}) + \sum_{n=1}^N \int d^3r' d^3r'' \vec{\mathbf{G}}(\mathbf{r}, \mathbf{r}') \cdot \vec{\mathbf{T}}(\mathbf{r}' - \mathbf{r}_n, \mathbf{r}'' - \mathbf{r}_n) \cdot \mathbf{E}_n^{\text{exc}}(\mathbf{r}''), \quad (3)$$

where $\mathbf{E}_n^{\text{exc}}$ is the exciting field at the n th particle and it is a function of \mathbf{r}'' . It is also a function of \mathbf{r}_n and of the position of all other scatterers. Although the range of integration in both integrals is over all space one has to recall that $\mathbf{T}(\mathbf{r}, \mathbf{r}')$ is zero whenever $\mathbf{r} \notin V_S$ or $\mathbf{r}' \notin V_S$.

For a given configuration of N particles we can set up a system of N equations for the N exciting fields at each particle:

$$\mathbf{E}_j^{\text{exc}}(\mathbf{r}) = \mathbf{E}^i(\mathbf{r}) + \sum_{n \neq j}^N \mathbf{E}_n^{\text{ind}}(\mathbf{r}), \quad (4)$$

for $j = 1 \dots N$. If one solves, in principle, this system of N integral equations and introduces the calculated exciting fields in Eq. (3), one will get the total electric field for that particular configuration of particles. To obtain the average field over all possible configurations, one must calculate the induced fields for all allowed configurations and average them weighted by the probability of each configuration. Obviously, the generation of the different possible configurations, as well as the probability of each configuration, will depend on the statistical characteristics of the specific physical system that one would like to simulate. Besides, an exact numerical calculation will be limited to a finite (and rather small) number of particles; it will be time consuming and would not provide much physical insight. It would not be suitable, for instance, for inversion algorithms to retrieve the optical parameters of a monolayer from experimental data in a sensing experiment. Clearly, for applications-oriented work it is attractive to have simple approximate models, preferably with results that can be expressed with closed-form expressions. To this end, we may try to average formally the equations above and solve them in some approximate scheme. By formally we mean that the configurations and their probability will be taken as given. Later on we will choose them for a specific system.

A. Configurational Averages

All statistical properties of a random system of N particles are specified by the N -dimensional probability density function $p(\mathbf{R})$ of finding the N particles in a specific configuration, where $\mathbf{R} = [\mathbf{r}_1, \mathbf{r}_2, \dots, \mathbf{r}_N]$ is the set of the coordinate vectors of the centers of the N particles. The configurational average of any given quantity is taken by integrating over all space on each of the N position-vectors $[\mathbf{r}_1, \mathbf{r}_2, \dots, \mathbf{r}_N]$ the quantity to be averaged times $p(\mathbf{R})$. Thus, the average of the electric field requires the evaluation of N volume integrals, and can be formally written as

$$\langle \mathbf{E}(\mathbf{r}) \rangle = \int d^3r_1 \int d^3r_2 \dots \int d^3r_N p(\mathbf{R}) \mathbf{E}(\mathbf{r}, \mathbf{R}), \quad (5)$$

where $\mathbf{E}(\mathbf{r}, \mathbf{R})$ is the electric field at \mathbf{r} for a specific configuration $\mathbf{R} = [\mathbf{r}_1, \mathbf{r}_2, \dots, \mathbf{r}_N]$. Then the average of the terms in Eq. (3) gives

$$\langle \mathbf{E}(\mathbf{r}) \rangle = \mathbf{E}^i(\mathbf{r}) + \sum_{n=1}^N \int \overset{\leftrightarrow}{\mathbf{G}}(\mathbf{r}, \mathbf{r}') \cdot \langle \overset{\leftrightarrow}{\mathbf{T}}(\mathbf{r}' - \mathbf{r}_n, \mathbf{r}'' - \mathbf{r}_n) \cdot \mathbf{E}_n^{\text{exc}}(\mathbf{r}'', \mathbf{R}) \rangle d^3 r' d^3 r''. \quad (6)$$

The term with the configurational average inside the integrand on the right-hand side of the latter equation can be calculated by taking first the conditional average of the term keeping the position of the n th scatterer fixed and then averaging over the position of the n th scatterer. That is, we can write

$$\begin{aligned} \langle \overset{\leftrightarrow}{\mathbf{T}}(\mathbf{r}' - \mathbf{r}_n, \mathbf{r}'' - \mathbf{r}_n) \cdot \mathbf{E}_n^{\text{exc}}(\mathbf{r}'', \mathbf{R}) \rangle &= \int d^3 r_n p(\mathbf{r}_n) \\ &\times \prod_{j \neq n}^N \int d^3 r_j p(\mathbf{R}|\mathbf{r}_n) \overset{\leftrightarrow}{\mathbf{T}}(\mathbf{r}' \\ &- \mathbf{r}_n, \mathbf{r}'' - \mathbf{r}_n) \cdot \mathbf{E}_n^{\text{exc}}(\mathbf{r}'', \mathbf{R}), \end{aligned} \quad (7)$$

where $p(\mathbf{R}|\mathbf{r}_n)$ is the conditional probability density function of finding a given configuration \mathbf{R} given that the n th scatterer is at \mathbf{r}_n . Since $\overset{\leftrightarrow}{\mathbf{T}}(\mathbf{r}' - \mathbf{r}_n, \mathbf{r}'' - \mathbf{r}_n)$ depends only on the position of the n th scatterer, it can be moved out from all integrals in the latter expression except the one over the position of the n th scatterer. We then write

$$\langle \overset{\leftrightarrow}{\mathbf{T}}(\mathbf{r}' - \mathbf{r}_n, \mathbf{r}'' - \mathbf{r}_n) \cdot \mathbf{E}_n^{\text{exc}}(\mathbf{r}'', \mathbf{R}) \rangle = \int d^3 r_n p(\mathbf{r}_n) \overset{\leftrightarrow}{\mathbf{T}}(\mathbf{r}' - \mathbf{r}_n, \mathbf{r}'' - \mathbf{r}_n) \cdot \langle \mathbf{E}_n^{\text{exc}}(\mathbf{r}'', \mathbf{R}) \rangle_n, \quad (8)$$

where $\langle \rangle_n$ denotes average with the n th scatterer fixed at \mathbf{r}_n . Note that

$$\langle \mathbf{E}_n^{\text{exc}}(\mathbf{r}'', \mathbf{R}) \rangle_n = \prod_{j \neq n}^N \int d^3 r_j p(\mathbf{R}|\mathbf{r}_n) \cdot \mathbf{E}_n^{\text{exc}}(\mathbf{r}'', \mathbf{R}) \quad (9)$$

is a function of \mathbf{r}'' and \mathbf{r}_n . In order to make this dependence more explicit we modify the notation and suppress in $\langle \mathbf{E}_n^{\text{exc}}(\mathbf{r}'', \mathbf{R}) \rangle_n$ the arguments inside the brackets and replace $\langle \mathbf{E}_n^{\text{exc}}(\mathbf{r}'', \mathbf{R}) \rangle_n$ by $\langle \mathbf{E}_n^{\text{exc}} \rangle_n(\mathbf{r}'', \mathbf{r}_n)$, where the dependence on the arguments stands explicitly outside the brackets.

We now assume a particular system of volume V in which the probability density of finding the center of any scatterer within this volume is uniform, that is, $p(\mathbf{r}_n) = 1/V$ for $\mathbf{r}_n \in V$ and is zero otherwise (and this is for all n). Thus the average $\langle \mathbf{E}_n^{\text{exc}} \rangle_n(\mathbf{r}'', \mathbf{r}_n)$ is the same for all particles and we can replace the sum in Eq. (6) by the factor N . Then, Eq. (6) becomes

$$\begin{aligned} \langle \mathbf{E}(\mathbf{r}) \rangle &= \mathbf{E}^i(\mathbf{r}) + \rho \int d^3 r' \overset{\leftrightarrow}{\mathbf{G}}(\mathbf{r}, \mathbf{r}') \int d^3 r'' \\ &\times \int d^3 r_n p(\mathbf{r}_n) \overset{\leftrightarrow}{\mathbf{T}}(\mathbf{r}' - \mathbf{r}_n, \mathbf{r}'' - \mathbf{r}_n) \cdot \langle \mathbf{E}_n^{\text{exc}} \rangle_n(\mathbf{r}'', \mathbf{r}_n), \end{aligned} \quad (10)$$

where $\rho = N/V$ is the particle number density.

Now, we must find an equation for the average exciting field. Averaging all terms in the system of equations in (5) gives

$$\begin{aligned} \langle \mathbf{E}_j^{\text{exc}}(\mathbf{r}, \mathbf{R}) \rangle_j &= \mathbf{E}^i(\mathbf{r}) + \int d^3 r' \overset{\leftrightarrow}{\mathbf{G}}(\mathbf{r}, \mathbf{r}') \\ &\cdot \int d^3 r'' \sum_{n \neq j}^N \langle \overset{\leftrightarrow}{\mathbf{T}}(\mathbf{r}' - \mathbf{r}_n, \mathbf{r}'' - \mathbf{r}_n) \cdot \langle \mathbf{E}_n^{\text{exc}}(\mathbf{r}'', \mathbf{R}) \rangle_{nj} \rangle_j, \end{aligned} \quad (11)$$

where $\langle \mathbf{E}_n^{\text{exc}}(\mathbf{r}'', \mathbf{R}) \rangle_{nj}$ means averaging holding fixed both, the j th particle at \mathbf{r}_j and the n th particle at \mathbf{r}_n . Note that

$$\begin{aligned} \langle \overset{\leftrightarrow}{\mathbf{T}}(\mathbf{r}' - \mathbf{r}_n, \mathbf{r}'' - \mathbf{r}_n) \cdot \langle \mathbf{E}_n^{\text{exc}}(\mathbf{r}'', \mathbf{R}) \rangle_{nj} \rangle_j \\ = \int d^3 r_n p(\mathbf{r}_n|\mathbf{r}_j) \overset{\leftrightarrow}{\mathbf{T}}(\mathbf{r}' - \mathbf{r}_n, \mathbf{r}'' - \mathbf{r}_n) \cdot \langle \mathbf{E}_n^{\text{exc}}(\mathbf{r}'', \mathbf{R}) \rangle_{nj}, \end{aligned} \quad (12)$$

where $p(\mathbf{r}_n|\mathbf{r}_j)$ is the conditional probability density function of finding the n th scatterer at \mathbf{r}_n given that the j th particle is at \mathbf{r}_j . We can write $p(\mathbf{r}_n|\mathbf{r}_j) = g(\mathbf{r}_n, \mathbf{r}_j)/(V - V_b) \cong g(\mathbf{r}_n, \mathbf{r}_j)/V$, where g is the so called two-particle correlation function (it is zero if either \mathbf{r}_n or \mathbf{r}_j are closer to each other than one particle diameter) and V_b is the exclusion volume of one particle ($V_b \ll V$).

We get

$$\begin{aligned} \langle \mathbf{E}_j^{\text{exc}}(\mathbf{r}, \mathbf{R}) \rangle_j &= \mathbf{E}^i(\mathbf{r}) + \int d^3 r' \overset{\leftrightarrow}{\mathbf{G}}(\mathbf{r}, \mathbf{r}') \\ &\cdot \int d^3 r'' \rho \int d^3 r_n g(\mathbf{r}_n, \mathbf{r}_j) \overset{\leftrightarrow}{\mathbf{T}}(\mathbf{r}' - \mathbf{r}_n, \mathbf{r}'' - \mathbf{r}_n) \\ &\cdot \langle \mathbf{E}_n^{\text{exc}}(\mathbf{r}'', \mathbf{R}) \rangle_{nj}, \end{aligned} \quad (13)$$

where we used $p(\mathbf{r}_n|\mathbf{r}_j) \cong g(\mathbf{r}_n, \mathbf{r}_j)/V$, replaced the sum $\sum_{n \neq j}^N$ by the factor $(N - 1)$, and then we took $(N - 1)/V \cong N/V = \rho$. Note that $\langle \mathbf{E}_j^{\text{exc}}(\mathbf{r}, \mathbf{R}) \rangle_j$ is a function of \mathbf{r} and \mathbf{r}_j only, whereas $\langle \mathbf{E}_n^{\text{exc}}(\mathbf{r}'', \mathbf{R}) \rangle_{nj}$ is a function of $\mathbf{r}'', \mathbf{r}_j$ and \mathbf{r}_n . Formally we can write

$$\langle \mathbf{E}_n^{\text{exc}}(\mathbf{r}'', \mathbf{R}) \rangle_{jn} = \prod_{m \neq n, j}^N \int d^3 r_m p(\mathbf{R}|\mathbf{r}_n, \mathbf{r}_j) \bar{\mathbf{E}}_n^{\text{exc}}(\mathbf{r}'', \mathbf{R}), \quad (14)$$

where $p(\mathbf{R}|\mathbf{r}_n, \mathbf{r}_j)$ is the density of conditional probability function of finding the configuration \mathbf{R} given that the n th and j th particles are kept fixed at \mathbf{r}_n and \mathbf{r}_j , respectively. Also, although the integrals over $d^3 r'$ and $d^3 r''$ in Eq. (13) extend over all space, the transition operator $\overset{\leftrightarrow}{\mathbf{T}}(\mathbf{r}' - \mathbf{r}_n, \mathbf{r}'' - \mathbf{r}_n)$ is zero whenever either of its arguments lies outside the volume occupied by the n th particle.

At this point we introduce the so called QCA (see for example [21,23,28,30,33]) by assuming

$$\langle \mathbf{E}_n^{\text{exc}}(\mathbf{r}, \mathbf{R}) \rangle_{nj} \cong \langle \mathbf{E}_n^{\text{exc}}(\mathbf{r}, \mathbf{R}) \rangle_n \equiv \langle \mathbf{E}_n^{\text{exc}} \rangle_n(\mathbf{r}, \mathbf{r}_n), \quad (15)$$

where we have used here the notation introduced after Eq. (9). To simplify the notation even further, let us remove the average signs and write explicitly only the arguments of the average exciting field within the QCA. That is, instead of $\langle \mathbf{E}_n^{\text{exc}} \rangle_n(\mathbf{r}, \mathbf{r}_n)$ one writes simply $\mathbf{E}_n^{\text{exc}}(\mathbf{r}, \mathbf{r}_n)$. Then, by substituting Eq. (15) into Eq. (13) one obtains a true integral equation for the unknown function $\mathbf{E}_n^{\text{exc}}(\mathbf{r}, \mathbf{r}_n)$, called the QCA integral equation, that can be written as,

$$\begin{aligned} \mathbf{E}_j^{\text{exc}}(\mathbf{r}, \mathbf{r}_j) = & \mathbf{E}^i(\mathbf{r}) + \int d^3r' \vec{\mathbf{G}}(\mathbf{r}, \mathbf{r}') \\ & \cdot \int d^3r'' \rho \int d^3r_n g(\mathbf{r}_n, \mathbf{r}_j) \vec{\mathbf{T}}(\mathbf{r}' - \mathbf{r}_n, \mathbf{r}'' - \mathbf{r}_n) \\ & \cdot \mathbf{E}_n^{\text{exc}}(\mathbf{r}'', \mathbf{r}_n), \end{aligned} \quad (16)$$

which in the case of spheres should be satisfied only for $|\mathbf{r} - \mathbf{r}_j| \leq a$ and note that $\mathbf{E}_n^{\text{exc}}(\mathbf{r}'', \mathbf{r}_n)$ is defined only for $|\mathbf{r}'' - \mathbf{r}_n| \leq a$.

As already said, we are interested in approximate solutions leading to simple analytical expressions valid for any size of particles and any angle of incidence. In the next section we develop such a model using Eq. (16) as a starting point.

3. MODEL FOR A FREE-STANDING MONOLAYER

We aim to develop a model for the coherent reflection and transmission of light from a monolayer of infinite extent composed by identical spherical particles of radius a , in which all particles have, on the average, the same surroundings. We will assume that the centers of all particles lie on the xy -plane as illustrated in Fig. 1. However, for the sake of generality and for future reference we will first assume that the center of all particles lie within a thin layer of width $\Delta z < a$ and finite area A . We assume there are N particles in the system and the area of their projection on the x - y plane is a fraction Θ of the area A and Θ is referred to as the surface-coverage fraction. When suitable we will take the limits $\Delta z \rightarrow 0$, $A \rightarrow \infty$ and $N \rightarrow \infty$ keeping Θ constant. Then, the volume V of space available to the centers of the particles (not to the whole particles) is $\Delta z \times A$. We will assume the area A is a square of sides $2L$ with the origin of coordinates placed at the center of the square, as shown in Fig. 1. Thus the integrals in Eq. (16) over dx_n and dy_n , the available location of the n th particle, are from $-L$ to $+L$ and we shall take the limit $L \rightarrow \infty$ to make the monolayer of infinite extent while keeping the coverage fixed.

Now, if the monolayer of infinite extent is illuminated by a plane wave, then the average exciting field for any given particle located at \mathbf{r}_p must depend only on $\mathbf{r} - \mathbf{r}_p$, except for a phase factor. This is because the system is statistically homo-

geneous ($p(\rightarrow r_n)$ is uniform within V), thus on the average, the surroundings of any given particle are equivalent and the only difference in the calculation of the average exciting field, is the difference in phase of the incident wave at the location of any given particle. In other words, if we calculate the exciting field for the p th particle while keeping the particle fixed at \mathbf{r}_p and obtain $\mathbf{E}_p^{\text{exc}}$, then relocating the particle along the xy -plane to $\mathbf{r}_p + \mathbf{s}_{\parallel}$ with $\mathbf{s}_{\parallel} = s_x \hat{\mathbf{a}}_x + s_y \hat{\mathbf{a}}_y$, and taking the average again, must yield the same field but multiplied by the phase factor $\exp[i\mathbf{k}_{\parallel}^i \cdot \mathbf{s}_{\parallel}]$. This is actually true only in the limit of a monolayer of infinite extent ($A \rightarrow \infty$). Only then all particles see on the average the same surroundings and there are no border effects. Therefore, we can write

$$\mathbf{E}_p^{\text{exc}}(\mathbf{r}, \mathbf{r}_p) = \exp[i\mathbf{k}_{\parallel}^i \cdot \mathbf{r}_p] \mathbf{F}(\mathbf{r} - \mathbf{r}_p), \quad (17)$$

for $p = 1, 2, \dots, N$ and $\mathbf{F}(\mathbf{r} - \mathbf{r}_p)$ is an electric field common to all particles.

We can write the fields $\mathbf{E}_j^{\text{exc}}$ and $\mathbf{E}_n^{\text{exc}}$ appearing in Eq. (16) in the form given in Eq. (17) replacing p by j and n accordingly. We then obtain an integral equation for the function $\mathbf{F}(\mathbf{r} - \mathbf{r}_p)$. Therefore, the calculation of the average electric field within the QCA is formally reduced to solving the resulting integral equation for the field factor $\mathbf{F}(\mathbf{r} - \mathbf{r}_p)$. Once we know F we can calculate the average electric field in Eq. (10) using the resulting exciting field given by Eq. (17).

A. Ansatz for the Exciting Field

In order to obtain a relatively simple and useful model for the coherent reflection and transmission coefficients of a free-standing monolayer we seek an approximate solution to the QCA integral equation [Eq. (16)] by assuming that F is given in terms of propagating plane waves.

We could start by assuming a single plane wave, $\mathbf{F}(\mathbf{r} - \mathbf{r}_p) = E_1 \exp[i\mathbf{k}_1 \cdot (\mathbf{r} - \mathbf{r}_p)] \hat{\mathbf{e}}_1$. However, when introduced on the right-hand side of Eq. (16) consistency cannot be achieved because after performing the indicated integrals, one obtains, among other contributions, another plane wave traveling in the specular direction. (This will become apparent below.) The specular direction in this case is the direction of a plane wave reflected specularly on the plane of the

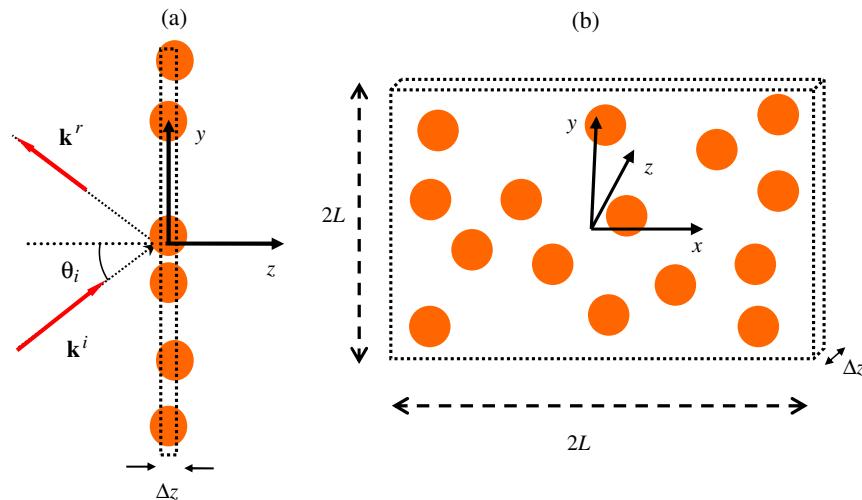


Fig. 1. (Color online) Sketch of the (a) side view and (b) top view of a free-standing monolayer of particles. The incident wave comes from $z < 0$ at an angle θ_i with respect to the monolayer's normal (the z -axis). The incident wave vector is assumed to be in the y - z plane.

monolayer, that is, the xy -plane. Thus the wavevector for the specularly reflected wave has the same wavevector components but with the sign of the z component changed. Therefore to obtain a consistent equation for F in the form of traveling plane waves, we have to assume that F is a sum of a plane wave plus a specularly reflected wave. Therefore our Ansatz to solve the integral equation for the function F is

$$\mathbf{F}(\mathbf{r} - \mathbf{r}_p) = E_1 \exp[i\mathbf{k}_1 \cdot (\mathbf{r} - \mathbf{r}_p)]\hat{\mathbf{e}}_1 + E_2 \exp[i\mathbf{k}_2 \cdot (\mathbf{r} - \mathbf{r}_p)]\hat{\mathbf{e}}_2, \quad (18a)$$

where $\mathbf{k}_1 = k_{1x}\hat{\mathbf{a}}_x + k_{1y}\hat{\mathbf{a}}_y + k_{1z}\hat{\mathbf{a}}_z$ and $\mathbf{k}_2 = k_{2x}\hat{\mathbf{a}}_x + k_{2y}\hat{\mathbf{a}}_y - k_{2z}\hat{\mathbf{a}}_z$. The exciting field at any of the particles is then of the form

$$\mathbf{E}_p^{\text{exc}}(\mathbf{r}, \mathbf{r}_p) = E_1 \exp[i(\mathbf{k}_1^i - \mathbf{k}_1) \cdot \mathbf{r}_p] \exp(i\mathbf{k}_1 \cdot \mathbf{r})\hat{\mathbf{e}}_1 + E_2 \exp[i(\mathbf{k}_1^i - \mathbf{k}_2) \cdot \mathbf{r}_p] \exp(i\mathbf{k}_2 \cdot \mathbf{r})\hat{\mathbf{e}}_2. \quad (18b)$$

Using this Ansatz in the right- and left-hand sides of Eq. (16) yields a consistency equation from which the unknowns, E_1 , E_2 , \mathbf{k}_1 , \mathbf{k}_2 , $\hat{\mathbf{e}}_1$, and $\hat{\mathbf{e}}_2$ can be determined.

B. Induced Fields

We will show in some detail the calculation of the second term on the right-hand side of Eq. (16) which involve multiple integrals. For simplicity in the presentation we will use here only one traveling plane wave, which could be either one in the Ansatz given in Eq. (18). At the end, we will add the contribution from both plane waves.

Thus, let us first consider, $\mathbf{F} = E_{\text{exc}} \exp[i\mathbf{k}^{\text{exc}} \cdot (\mathbf{r} - \mathbf{r}_p)]\hat{\mathbf{e}}_{\text{exc}}$, where E_{exc} , \mathbf{k}^{exc} , and $\hat{\mathbf{e}}_{\text{exc}}$ can be either E_1 , \mathbf{k}_1 and $\hat{\mathbf{e}}_1$, or E_2 , \mathbf{k}_2 , and $\hat{\mathbf{e}}_2$. From Eq. (17) we get, $\mathbf{E}_p^{\text{exc}}(\mathbf{r}, \mathbf{r}_p) = E_{\text{exc}} \exp[i\mathbf{k}_p \cdot \mathbf{r}_p] \exp(i\mathbf{k}^{\text{exc}} \cdot \mathbf{r})\mathbf{e}_{\text{exc}}$, where $\mathbf{k}_p \equiv (\mathbf{k}_1^i - \mathbf{k}^{\text{exc}})$. We will assume that the centers of all the particles lie with uniform density of probability within a thin layer in space of width Δz and area $2L \times 2L$. We should remark that the centers of all particles are contained within Δz although the particles themselves extend outside Δz . When suitable we take the limit $\Delta z \rightarrow 0$ and $L \rightarrow \infty$ to define a strictly flat monolayer of infinite extent.

For simplicity we will assume the particle correlation function is a correlation hole; this means it is unity except within a sphere or radius $2a$ around \mathbf{r}_j , where it is zero.

$$g(\mathbf{r}_j - \mathbf{r}_n) = \begin{cases} 0 & \text{if } |\mathbf{r}_j - \mathbf{r}_n| < 2a \\ 1 & \text{if } |\mathbf{r}_j - \mathbf{r}_n| > 2a \end{cases}. \quad (19)$$

This assumption is a good approximation only for moderately small density of particles. When the density of particles is not small, even if there is no interaction among the particles except for being impenetrable (hard sphere), some ordering of the particles arises. For instance, for closest packing of the particles, the particles touch each other and the distance between the center of one particle and its nearest neighbors is one diameter. We will not find any particles with their centers at a distance slightly larger than one diameter. Thus, for larger densities, the two-particle correlation function is still equal to zero for $|\mathbf{r}_j - \mathbf{r}_n| < 2a$, but for $|\mathbf{r}_j - \mathbf{r}_n| > 2a$ it has oscillations around the value one, with decreasing amplitudes as $|\mathbf{r}_j - \mathbf{r}_n|$ increases. For higher density of particles one can use an ana-

lytical approximation to the pair-correlation function such as the Percus–Yevick one [34] or simply generate it numerically from a Monte Carlo simulation [35]. Actually, for even higher densities the three-particle correlation function may be needed [33].

Now, to perform the integrals in the right-hand side of Eq. (16) with an exciting field in the form of a plane wave, it is convenient to express the transition operator in terms of its momentum representation,

$$\vec{\mathbf{T}}(\mathbf{r}', \mathbf{r}'') = \frac{1}{(2\pi)^6} \int d^3p' \int d^3p'' \exp(i\mathbf{p}' \cdot \mathbf{r}') \vec{\mathbf{T}}(\mathbf{p}', \mathbf{p}'') \times \exp(-i\mathbf{p}'' \cdot \mathbf{r}''), \quad (20)$$

and use a plane-wave expansion of the dyadic Green's function $\mathbf{G}(\mathbf{r}, \mathbf{r}')$ which will be displayed below. Here, in order to avoid a cumbersome notation, we use the same symbol for the transition operator \mathbf{T} in its space and momentum representations, the difference between them will be indicated only through its arguments. The latter plane-wave expansion changes discontinuously at some plane passing through the observation point. The orientation in space of such plane depends on how we choose the plane wave expansion. It is convenient to divide the integral over d^3r_n throughout the volume V in the right-hand side of Eq. (16) in four parts as indicated in Fig. 2b. In each region shown in Fig. 2b we should use a different plane wave expansion of $\mathbf{G}(\mathbf{r}, \mathbf{r}')$ such that when performing the integrals in Eq. (16) in any of these regions the discontinuity in the plane wave expansion does not contribute. The reason behind choosing the particular division shown in Fig. 2 is that we are assuming that the wave incident to the monolayer travels in the zy -plane ($k_x^i = 0$). In the case of a monolayer of infinite extent the average scattered waves turn out (as one would expect) to be on the same plane, and thus, the corresponding wave vectors have their x -component also equal to zero. Therefore, the integrals leading to the main

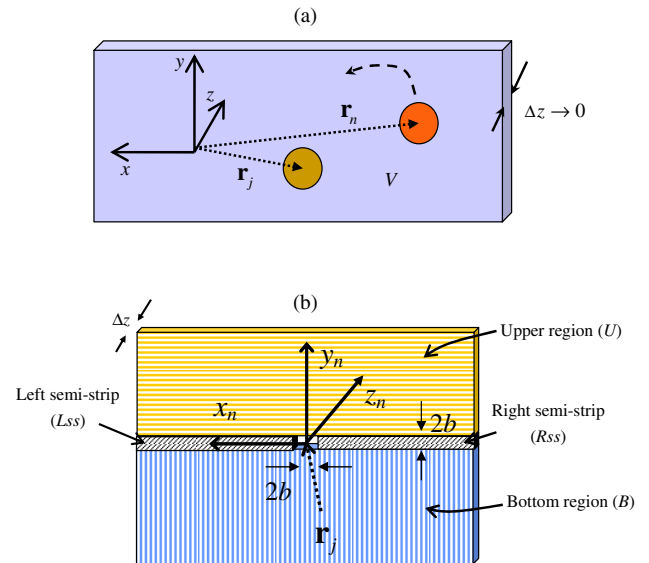


Fig. 2. (Color online) (a) Illustration of the averaging procedure keeping the j th particle fixed at \mathbf{r}_j and moving the n th particle across the plane of the monolayer, except where $|\mathbf{r}_j - \mathbf{r}_n| < 2a$. (b) Different sections of the monolayer plane in which we divide the integral over d^3r_n around \mathbf{r}_j .

contributions to the induced fields simplify with the division shown in Fig. 2.

Thus, let us split the integral over d^3r_n in two contributions, one from the bottom (B) region of the monolayer plane defined by all points \mathbf{r}_n for which $y_j - y_n > 2a$ and the other one from the top (T) region formed by all points \mathbf{r}_n with $y_j - y_n < 2a$ (see Fig. 2). These contributions correspond to the integrals

$$\int_B d^3r_n(\cdot) \rightarrow \int_0^{\Delta z} \int_{-L}^{y_j-2a} \int_{-L}^L dx_n dy_n dz_n(\cdot) \quad \text{and} \\ \int_T d^3r_n(\cdot) \rightarrow \int_0^{\Delta z} \int_{y_j+2a}^L \int_{-L}^L dx_n dy_n dz_n(\cdot),$$

where we will take the limits $\Delta z \rightarrow 0$ and $L \rightarrow \infty$ when convenient. The contributions from the remaining side strips, the right and left semistrips shown in Fig. 2 where $|y_j - y_n| < 2a$ can be neglected. This is justified in Appendix A.

To calculate the contributions from the bottom and top regions we should use the following plane wave expansion of the dyadic Green's function:

$$\vec{\mathbf{G}}_{\pm}(\mathbf{r}, \mathbf{r}') = -\hat{\mathbf{a}}_y \hat{\mathbf{a}}_y \delta(\mathbf{r} - \mathbf{r}') + \frac{i}{2} \iint \frac{dk_x^s dk_z^s}{(2\pi)^2} \frac{1}{k_y^s} (\mathbf{I} - \hat{\mathbf{k}}_{\pm}^s \hat{\mathbf{k}}_{\pm}^s) \\ \cdot \exp[i\mathbf{k}_{\pm}^s \cdot (\mathbf{r} - \mathbf{r}')], \quad (21)$$

where $\mathbf{k}_{\pm}^s = k_x^s \hat{\mathbf{a}}_x \pm k_y^s \hat{\mathbf{a}}_y + k_z^s \hat{\mathbf{a}}_z$, $k_y^s = \sqrt{k_m^2 - (k_x^s)^2 - (k_z^s)^2}$ (this is the positive root) and $\hat{\mathbf{k}}_{\pm}^s = \mathbf{k}_{\pm}^s / |\mathbf{k}_{\pm}^s|$ is a unit vector and the sign “+” is $y > y'$, whereas the “-” sign is for $y < y'$. (See [36], pages 381–384.) We recall that $\hat{\mathbf{a}}_x$, $\hat{\mathbf{a}}_y$, and $\hat{\mathbf{a}}_z$ are unit vectors along the Cartesian x , y , and z axes, and the term with the delta function in the right-hand side of Eq. (21) will take care of the contributions of the singularities of $\vec{\mathbf{G}}_{\pm}$ in the source region while performing the integral in Eq. (16).

Using $\mathbf{E}_n^{\text{exc}}(\mathbf{r}, \mathbf{r}_n) = E_{\text{exc}} \exp[i\mathbf{k}_D \cdot \mathbf{r}_n] \exp(i\mathbf{k}^{\text{exc}} \cdot \mathbf{r}) \hat{\mathbf{e}}_{\text{exc}}$ and Eqs. (20) and (21) in the right-hand side of Eq. (16) yields

$$\mathbf{E}_j^{\text{exc}}(\mathbf{r}, \mathbf{r}_j) = \mathbf{E}^i(\mathbf{r}) + \frac{i\rho}{2} E_{\text{exc}} \int d^3r' \iint \frac{dk_x^s dk_z^s}{(2\pi)^2} \frac{1}{k_y^s} (\mathbf{I} - \hat{\mathbf{k}}_{\pm}^s \hat{\mathbf{k}}_{\pm}^s) \\ \cdot \exp[i\mathbf{k}_{\pm}^s \cdot (\mathbf{r} - \mathbf{r}')] \int d^3r'' \int \frac{d^3p'}{(2\pi)^3} \int \frac{d^3p''}{(2\pi)^3} \\ \times \int d^3r_n g(|\mathbf{r}_j - \mathbf{r}_n|) \exp(i\mathbf{p}' \cdot [\mathbf{r}' - \mathbf{r}_n]) \vec{\mathbf{T}}(\mathbf{p}', \mathbf{p}'') \\ \cdot \exp(-i\mathbf{p}'' \cdot [\mathbf{r}'' - \mathbf{r}_n]) \exp(i\mathbf{k}_D \cdot \mathbf{r}_n) \\ \times \exp(i\mathbf{k}^{\text{exc}} \cdot \mathbf{r}') \hat{\mathbf{e}}_{\text{exc}}, \quad (22)$$

where the choice of \mathbf{k}_{\pm}^s or \mathbf{k}_{\mp}^s will be determined when performing the integrals. Note that the contribution to $\mathbf{E}_j^{\text{exc}}(\mathbf{r}, \mathbf{r}_j)$ of the term with a Dirac's delta function in the expansion of $\vec{\mathbf{G}}(\mathbf{r}, \mathbf{r}')$, is obtained by substituting Eq. (21) directly into Eq. (16). If one uses $\vec{\sigma} = (1/i\omega\mu_0)\mathbf{T}$ and Eq. (2a), this term can be written as $-i\omega\mu_0\rho\hat{\mathbf{a}}_y\hat{\mathbf{a}}_y \cdot \int d^3r_n g(\mathbf{r}_n, \mathbf{r}_j) \mathbf{J}_{\text{ind}}^{(n)}(\mathbf{r} - \mathbf{r}_n)$, where $\mathbf{J}_{\text{ind}}^{(n)}(\mathbf{r} - \mathbf{r}_n)$ is the current density induced at \mathbf{r} by a sphere whose center is located at \mathbf{r}_n and it is different from zero only for $|\mathbf{r} - \mathbf{r}_n| < a$. Since the relevant values of \mathbf{r} in $\mathbf{E}_j^{\text{exc}}(\mathbf{r}, \mathbf{r}_j)$ are restricted to $|\mathbf{r} - \mathbf{r}_j| < a$, but \mathbf{r}_n cannot get close to \mathbf{r}_j , for $|\mathbf{r}_n - \mathbf{r}_j| < 2a$, due to the presence of $g(\mathbf{r}_n, \mathbf{r}_j)$, this term will vanish.

In Eq. (22) when we integrate over d^3r_n throughout the bottom region of the monolayer plane we must choose the “+” sign in \mathbf{k}_{\pm}^s whereas when integrating over the top region we must choose the “-” sign. We can perform the integrals over d^3r'' and d^3r' which give the factors $(2\pi)^3\delta(\mathbf{p}'' - \mathbf{k}^{\text{exc}})$ and $(2\pi)^3\delta(\mathbf{p}' - \mathbf{k}_{\pm}^s)$, respectively. To perform the integral over d^3r' we choose either \mathbf{k}_{\pm}^s or \mathbf{k}_{\mp}^s (in the bottom or top integration regions, respectively), which assumes that $y - y' > 0$ or $y - y' < 0$. This is again possible because the transition operator is zero whenever $|\mathbf{r}' - \mathbf{r}_n| > a$ or $|\mathbf{r}'' - \mathbf{r}_n| > a$ and for any two vectors \mathbf{r}_j and \mathbf{r}_n that satisfy $y_j - y_n > 2a$ or $y_j - y_n < 2a$ we have that $y - y' > 0$ or $y - y' < 0$, respectively, when the integrand is different from zero.

After performing the integrals over d^3r'' and d^3r' , the integrals over d^3p' and d^3p'' are trivial. We get

$$\mathbf{E}_j^{\text{exc}}(\mathbf{r}, \mathbf{r}_j) = \mathbf{E}^i(\mathbf{r}) + \frac{i\rho}{2} E_{\text{exc}} \iint \frac{dk_x^s dk_z^s}{(2\pi)^2} \frac{1}{k_y^s} (\mathbf{I} - \hat{\mathbf{k}}_{\pm}^s \hat{\mathbf{k}}_{\pm}^s) \\ \cdot \exp[i\mathbf{k}_{\pm}^s \cdot \mathbf{r}] \\ \times \int d^3r_n g(|\mathbf{r}_j - \mathbf{r}_n|) \exp(-i\mathbf{k}_{\pm}^s \cdot \mathbf{r}_n) \vec{\mathbf{T}}(\mathbf{k}_{\pm}^s, \mathbf{k}^{\text{exc}}) \\ \cdot \exp(i\mathbf{k}_{\parallel}^i \cdot \mathbf{r}_n) \hat{\mathbf{e}}_{\text{exc}}. \quad (23)$$

Now we can perform the integrals over d^3r_n on the bottom and top regions (B and T). In either half-plane the integral over dz_n gives a factor Δz in the limit $\Delta z \rightarrow 0$. The integral over dx_n , in the limit $L \rightarrow \infty$, gives the factor $(2\pi)\delta(k_x^s - k_x^i)$. But, for simplicity, we have chosen our coordinate axes such that $k_x^i = 0$, thus the integral over dx_n gives $(2\pi)\delta(k_x^s)$. Because of the latter delta function, the integral over dk_x^s is trivial.

We will now refer to the second term in the right-hand side of Eq. (23) as the “induced field exciting the j th particle” and denote it as $\mathbf{E}_j^{\text{ind}}(\mathbf{r})$. Since, as already said, we neglect the contributions from the integration d^3r_n over the side semistrips depicted in Fig. 2 (see Appendix A), we write $\mathbf{E}_j^{\text{ind}}(\mathbf{r})$ as the sum of only two terms, namely the integral over d^3r_n over the bottom region, $\mathbf{E}_B^{\text{ind}}(\mathbf{r}, \mathbf{r}_j)$, and that, over the top region, $\mathbf{E}_T^{\text{ind}}(\mathbf{r}, \mathbf{r}_j)$. Neglecting the contributions from the mentioned side-strips, $\mathbf{E}_j^{\text{ind}}(\mathbf{r})$ is well defined for $y_j - 2a < y < y_j + 2a$ and we then have

$$\mathbf{E}_j^{\text{ind}}(\mathbf{r}, \mathbf{r}_j) = \mathbf{E}_B^{\text{ind}}(\mathbf{r}, \mathbf{r}_j) + \mathbf{E}_T^{\text{ind}}(\mathbf{r}, \mathbf{r}_j), \quad (24)$$

where

$$\mathbf{E}_B^{\text{ind}}(\mathbf{r}, \mathbf{r}_j) = \frac{i\rho_s}{2} E_{\text{exc}} \int \frac{dk_z^s}{2\pi} \frac{1}{k_y^s} (\mathbf{I} - \hat{\mathbf{k}}_{+}^s \hat{\mathbf{k}}_{+}^s) \cdot \vec{\mathbf{T}}(\mathbf{k}_{+}^s, \mathbf{k}^{\text{exc}}) \\ \cdot \hat{\mathbf{e}}_{\text{exc}} \exp[i\mathbf{k}_{+}^s \cdot \mathbf{r}] \int_{-L}^{y_j-2a} dy_n \exp[i(k_y^i - k_y^s)y_n], \quad (25)$$

$$\mathbf{E}_T^{\text{ind}}(\mathbf{r}, \mathbf{r}_j) = \frac{i\rho_s}{2} E_{\text{exc}} \int \frac{dk_z^s}{2\pi} \frac{1}{k_y^s} (\mathbf{I} - \hat{\mathbf{k}}_{-}^s \hat{\mathbf{k}}_{-}^s) \cdot \vec{\mathbf{T}}(\mathbf{k}_{-}^s, \mathbf{k}^{\text{exc}}) \\ \cdot \hat{\mathbf{e}}_{\text{exc}} \exp[i\mathbf{k}_{-}^s \cdot \mathbf{r}] \int_{y_j+2a}^L dy_n \exp[i(k_y^i + k_y^s)y_n]. \quad (26)$$

where now $k_y^s = \sqrt{k_m^2 - (k_z^s)^2}$ and we used $\rho_s = \rho \Delta z = N \Delta z / V = N / A$. Recall that N is the number of particles in the system, V the volume of space where their centers lie, and $V = A \Delta z$ where the area $A = 4L^2$ is the area of the monolayer.

Performing the integral over dy_n yields

$$\begin{aligned} \mathbf{E}_B^{\text{ind}}(\mathbf{r}, \mathbf{r}_j) &= \frac{i\rho_s}{2} E_{\text{exc}} \int \frac{dk_z^s}{2\pi} \frac{(i4\pi/k_m) \mathbf{S}(\mathbf{k}_+^s, \mathbf{k}^{\text{exc}})}{k_y^s} \\ &\times \frac{\exp[i(k_y^i - k_y^s)(y_j - 2a)] - \exp[-i(k_y^i - k_y^s)L]}{i(k_y^i - k_y^s)} \\ &\times \exp[i\mathbf{k}_+^s \cdot \mathbf{r}], \end{aligned} \quad (27)$$

and

$$\begin{aligned} \mathbf{E}_T^{\text{ind}}(\mathbf{r}, \mathbf{r}_j) &= \frac{i\rho_s}{2} E_{\text{exc}} \int \frac{dk_z^s}{2\pi} \frac{(i4\pi/k_m) \mathbf{S}(\mathbf{k}_-^s, \mathbf{k}^{\text{exc}})}{k_y^s} \\ &\times \frac{\exp[i(k_y^i + k_y^s)L] - \exp[i(k_y^i + k_y^s)(y_j + 2a)]}{i(k_y^i + k_y^s)} \\ &\times \exp[i\mathbf{k}_-^s \cdot \mathbf{r}], \end{aligned} \quad (28)$$

where for economy and later convenience we defined

$$\mathbf{S}(\mathbf{q}, \mathbf{p}) \equiv \frac{k_m}{i4\pi} (\hat{\mathbf{I}} - \hat{\mathbf{q}} \hat{\mathbf{q}}) \cdot \hat{\mathbf{T}}(\mathbf{q}, \mathbf{p}) \cdot \hat{\mathbf{e}}_p. \quad (29)$$

In Appendix B we show that $\mathbf{E}_B^{\text{ind}}$ is given by

$$\begin{aligned} \mathbf{E}_B^{\text{ind}}(\mathbf{r}, \mathbf{r}_j) &= -\frac{1}{2} \alpha E_{\text{exc}} [\mathbf{S}(\mathbf{k}^i, \mathbf{k}^{\text{exc}}) \exp(i\mathbf{k}^i \cdot \mathbf{r}) \\ &+ \mathbf{S}(\mathbf{k}^r, \mathbf{k}^{\text{exc}}) \exp(i\mathbf{k}^r \cdot \mathbf{r})] - \rho_s \eta_B^{C_3}(\mathbf{r}) - \rho_s \eta_B^{-C_3}(\mathbf{r}), \end{aligned} \quad (30)$$

where $\alpha = 2\pi\rho_s/(k_m k_z^i)$, $\mathbf{k}^r = k_y^i \hat{\mathbf{a}}_y - k_z^i \hat{\mathbf{a}}_z$ is the wave vector of a specularly reflected wave from the plane of the monolayer, and the fields $\rho_s \eta_B^{C_3}(\mathbf{r})$ and $\rho_s \eta_B^{-C_3}(\mathbf{r})$ involve the integral of only evanescent fields. The superscripts C_3 and $-C_3$ denote integration contours in the complex plane. We also show in Appendix B that the average induced field coming from the top region of the monolayer yields two terms which involve the integrals of only evanescent fields and are proportional to the surface density of particles. That is,

$$\mathbf{E}_T^{\text{ind}}(\mathbf{r}, \mathbf{r}_j) = -\rho_s \eta_T^{C_3}(\mathbf{r}) - \rho_s \eta_T^{-C_3}(\mathbf{r}), \quad (31)$$

where the terms $\rho_s \eta_T^{C_3}(\mathbf{r})$ and $\rho_s \eta_T^{-C_3}(\mathbf{r})$ are given in Appendix B. Therefore, the induced field exciting the j th particle arising from the exciting plane wave is given by

$$\begin{aligned} \mathbf{E}_j^{\text{ind}}(\mathbf{r}, \mathbf{r}_j) &= -\frac{\alpha}{2} E_{\text{exc}} [\mathbf{S}(\mathbf{k}^i, \mathbf{k}^{\text{exc}}) \exp(i\mathbf{k}^i \cdot \mathbf{r}) \\ &+ \mathbf{S}(\mathbf{k}^r, \mathbf{k}^{\text{exc}}) \exp(i\mathbf{k}^r \cdot \mathbf{r})] - \rho_s \eta_{\text{evanes}}(\mathbf{r}), \end{aligned} \quad (32)$$

where $\eta_{\text{evan}}(\mathbf{r}) = \eta_B^{C_3}(\mathbf{r}) + \eta_B^{-C_3}(\mathbf{r}) + \eta_T^{C_3}(\mathbf{r}) + \eta_T^{-C_3}(\mathbf{r})$ is the sum of all the terms involving integrals of only evanescent fields.

Now, according to our Ansatz given in Eq. (18b), the induced field exciting the j th particle is obtained by adding the fields obtained above upon substitution of $E_{\text{exc}} = E_1$, $\mathbf{k}^{\text{exc}} = \mathbf{k}_1$, $\hat{\mathbf{e}}_{\text{exc}} = \hat{\mathbf{e}}_1$ and $E_{\text{exc}} = E_2$, $\mathbf{k}^{\text{exc}} = \mathbf{k}_2$, $\hat{\mathbf{e}}_{\text{exc}} = \hat{\mathbf{e}}_2$ in Eq. (32). We get

$$\begin{aligned} \mathbf{E}_j^{\text{ind}}(\mathbf{r}, \mathbf{r}_j) &= -\frac{\alpha}{2} E_1 [\mathbf{S}(\mathbf{k}^i, \mathbf{k}_1) \exp(\mathbf{k}^i \cdot \mathbf{r}) + \mathbf{S}(\mathbf{k}^r, \mathbf{k}_1) \exp(i\mathbf{k}^r \cdot \mathbf{r})] \\ &- \frac{\alpha}{2} E_2 [\mathbf{S}(\mathbf{k}^i, \mathbf{k}_2) \exp(\mathbf{k}^i \cdot \mathbf{r}) + \mathbf{S}(\mathbf{k}^r, \mathbf{k}_2) \exp(i\mathbf{k}^r \cdot \mathbf{r})] \\ &- \rho_s \eta_{\text{evanes}}^{(1)}(\mathbf{r}) - \rho_s \eta_{\text{evanes}}^{(2)}(\mathbf{r}), \end{aligned} \quad (33)$$

where we added the superscripts (1) and (2) to the contributions coming from the evanescent fields.

C. Consistency Equations

If we use Eq. (18b) to express the exciting field for the j th particle in the left hand side of Eq. (16) and replace the second term in the right-hand side of this same equation with the result in Eq. (33), we obtain a set of consistency equations for the unknown parameters in the assumed exciting field: E_1 , E_2 , \mathbf{k}_1 , $\hat{\mathbf{e}}_1$, \mathbf{k}_2 , and $\hat{\mathbf{e}}_2$. Note, however, that the factor $\alpha = 2\pi\rho_s/(k_m k_z^i) = 2\pi\rho_s/(k_m^2 \cos \theta_i)$ appearing in the induced fields diverges as the angle of incidence increases and approaches $\pi/2$. Thus, even for small ρ_s the factor α may not be small. Thus it is not possible to seek for a solution to the consistency equation in the form of a power series in ρ_s that would remain valid at all angles of incidence.

We can obtain a closed consistency equation which we can solve exactly for E_1 , E_2 , \mathbf{k}_1 , $\hat{\mathbf{e}}_1$, \mathbf{k}_2 , and $\hat{\mathbf{e}}_2$, if we drop the evanescent field terms, $\rho_s \eta_{\text{evanes}}^{(1)}(\mathbf{r})$ and $\rho_s \eta_{\text{evanes}}^{(2)}(\mathbf{r})$ given in Appendix B and appearing in the right-hand side of Eq. (33). We can justify this approximation by noting that, if we iterate the result by adding these terms to our Ansatz and repeat the whole procedure, we would arrive to the same equation but with the terms, $\rho_s \eta_{\text{evanes}}^{(1)}(\mathbf{r})$ and $\rho_s \eta_{\text{evanes}}^{(2)}(\mathbf{r})$, replaced by new ones. These new terms would be of second-order in the surface density of particles and thus, they will presumably be smaller. Also, iterating the Kernel of the integrals defining $\eta_{\text{evanes}}^{(1)}(\mathbf{r})$ and $\eta_{\text{evanes}}^{(2)}(\mathbf{r})$ in Appendix B, through all the procedure delineated in the same Appendix B, it is not difficult to see that these new terms would also consist only of evanescent fields.

Then, neglecting the evanescent-field terms in Eq. (33) and substituting the remaining terms for the second term in the right-hand side of Eq. (16) and using Eq. (18b) on the left-hand side of this same equation, yields the desired consistency equation. Equating terms with the same dependence on \mathbf{r} in both sides of the obtained equation requires $\mathbf{k}_1 = \mathbf{k}^i$, $\hat{\mathbf{e}}_1 = \hat{\mathbf{e}}_i$ and $\mathbf{k}_2 = \mathbf{k}^r$, $\hat{\mathbf{e}}_2 = \hat{\mathbf{e}}_r$, where $\hat{\mathbf{e}}_r$ is the polarization vector of the specularly reflected wave from the plane of the monolayer (which depends on $\hat{\mathbf{e}}_i$ as indicated below). Then, the exciting field at any particle is of the form

$$\mathbf{E}_p^{\text{exc}}(\mathbf{r}, \mathbf{r}_p) = E_1 \exp(i\mathbf{k}^i \cdot \mathbf{r}) \mathbf{e}_i + E_2 \exp(i\mathbf{k}^r \cdot \mathbf{r}) \mathbf{e}_r, \quad (34)$$

and we are left with two consistency equations for the remaining two unknowns E_1 and E_2 ,

$$E_1 \hat{\mathbf{e}}_i = E_i \hat{\mathbf{e}}_i - \frac{\alpha}{2} E_1 \mathbf{S}(\mathbf{k}^i, \mathbf{k}^i) - \frac{\alpha}{2} E_2 \mathbf{S}(\mathbf{k}^i, \mathbf{k}^r), \quad (35a)$$

and

$$E_2 \hat{\mathbf{e}}_r = -\frac{\alpha}{2} E_1 \mathbf{S}(\mathbf{k}^r, \mathbf{k}^i) - \frac{\alpha}{2} E_2 \mathbf{S}(\mathbf{k}^r, \mathbf{k}^r). \quad (35b)$$

where $\mathbf{S}(\mathbf{k}^r, \mathbf{k}^i)$ and $\mathbf{S}(\mathbf{k}^r, \mathbf{k}^r)$ are given by Eq. (29). To solve for E_1 and E_2 we take the scalar product of both sides of the first

and second equations with $\hat{\mathbf{e}}_i$ and $\hat{\mathbf{e}}_r$, respectively. Solving the obtained algebraic equations and noting that $\hat{\mathbf{e}}_i \cdot \mathbf{S}(\mathbf{k}^i, \mathbf{k}^i) = \hat{\mathbf{e}}_r \cdot \mathbf{S}(\mathbf{k}^r, \mathbf{k}^r)$ and $\hat{\mathbf{e}}_r \cdot \mathbf{S}(\mathbf{k}^r, \mathbf{k}^i) = \hat{\mathbf{e}}_i \cdot \mathbf{S}(\mathbf{k}^i, \mathbf{k}^r)$ yields

$$E_1 = \frac{E_i \left(1 + \frac{\alpha}{2} \hat{\mathbf{e}}_r \cdot \mathbf{S}(\mathbf{k}^r, \mathbf{k}^r) \right)}{1 + \alpha \hat{\mathbf{e}}_i \cdot \mathbf{S}(\mathbf{k}^i, \mathbf{k}^i) + \frac{\alpha^2}{4} [\hat{\mathbf{e}}_i \cdot \mathbf{S}(\mathbf{k}^i, \mathbf{k}^i)]^2 - \frac{\alpha^2}{4} [\hat{\mathbf{e}}_r \cdot \mathbf{S}(\mathbf{k}^r, \mathbf{k}^i)]^2}, \quad (36)$$

and

$$E_2 = \frac{-E_i \frac{\alpha}{2} \hat{\mathbf{e}}_r \cdot \mathbf{S}(\mathbf{k}^r, \mathbf{k}^i)}{1 + \alpha \hat{\mathbf{e}}_i \cdot \mathbf{S}(\mathbf{k}^i, \mathbf{k}^i) + \frac{\alpha^2}{4} [\hat{\mathbf{e}}_i \cdot \mathbf{S}(\mathbf{k}^i, \mathbf{k}^i)]^2 - \frac{\alpha^2}{4} [\hat{\mathbf{e}}_r \cdot \mathbf{S}(\mathbf{k}^r, \mathbf{k}^i)]^2}. \quad (37)$$

We can write the coefficient $\alpha = 2\pi\rho_s/(k_m k_z^i)$ as

$$\alpha = \frac{2\Theta}{x_m^2 \cos \theta_i}, \quad (38)$$

where Θ is the surface-coverage-fraction of the monolayer and $x_m = k_m a$ is the so called size parameter of the particle. To obtain the latter relation we used $\rho_s = N/A = N\pi a^2/(A\pi a^2) = \Theta/(\pi a^2)$.

D. Average Reflected and Transmitted Fields

Here we use Eq. (10), with the exciting field given in Eq. (34), to calculate the average reflected ($z < a$) and transmitted ($z > a$) fields. In this case it is convenient to expand the dyadic Green's function in plane waves traveling along the $+z$ or $-z$ depending on whether we are calculating the transmitted or reflected average wave, respectively. That is, we use

$$\begin{aligned} \overleftrightarrow{\mathbf{G}}_{\pm}(\mathbf{r}, \mathbf{r}') &= -\hat{\mathbf{a}}_z \hat{\mathbf{a}}_z \delta(\mathbf{r} - \mathbf{r}') + \frac{i}{2} \iint \frac{dk_x^s dk_y^s}{(2\pi)^2} \frac{1}{k_z^s} (\overleftrightarrow{\mathbf{I}} - \hat{\mathbf{k}}_{\pm}^s \hat{\mathbf{k}}_{\pm}^s) \\ &\cdot \exp[i\mathbf{k}_{\pm}^s \cdot (\mathbf{r} - \mathbf{r}')], \end{aligned} \quad (39)$$

where $\mathbf{k}_{\pm}^s = k_x^s \hat{\mathbf{a}}_x + k_y^s \hat{\mathbf{a}}_y \pm k_z^s \hat{\mathbf{a}}_z$, $k_z^s = \sqrt{k_m^2 - (k_x^s)^2 - (k_y^s)^2}$ and $\hat{\mathbf{k}}_{\pm}^s = \mathbf{k}_{\pm}^s/|\mathbf{k}_{\pm}^s|$ is a unit vector (e.g., see [36], pages 381–284). We should use the upper sign “(+)” for the transmitted average field when $z > a$ and the lower one “(–)” for the reflected average wave when $z < a$. In Appendix C we show that the transmitted field for $z > a$ is given by

$$\mathbf{E}_t(\mathbf{r}) = [E_i \mathbf{e}_i - \alpha E_1 \mathbf{S}(\mathbf{k}^i, \mathbf{k}^i) - \alpha E_2 \mathbf{S}(\mathbf{k}^i, \mathbf{k}^r)] \exp(i\mathbf{k}^i \cdot \mathbf{r}), \quad (40)$$

whereas the reflected field for $z < a$ is given by

$$\mathbf{E}_r(\mathbf{r}) = -\alpha [E_1 \mathbf{S}(\mathbf{k}^r, \mathbf{k}^i) + E_2 \mathbf{S}(\mathbf{k}^r, \mathbf{k}^r)] \exp(i\mathbf{k}^r \cdot \mathbf{r}). \quad (41)$$

We define the coherent transmission (t_{coh}) and reflection (r_{coh}) coefficients such that $E_t = t_{\text{coh}} E_i$ and $E_r = r_{\text{coh}} E_i$. Using these latter expressions and Eqs. (36) and (37) in Eqs. (40) and (41) yield the desired expressions for t_{coh} and r_{coh} . The results are expressed in a more appealing and transparent form by using the following identities

$$\mathbf{S}(\mathbf{k}^i, \mathbf{k}^i) = \frac{k_m}{4\pi i} (\overleftrightarrow{\mathbf{I}} - \hat{\mathbf{k}}^i \hat{\mathbf{k}}^i) \cdot \overleftrightarrow{\mathbf{T}}(\mathbf{k}^i, \mathbf{k}^i) \cdot \hat{\mathbf{e}}_i = S(0) \hat{\mathbf{e}}_i, \quad (43a)$$

$$\mathbf{S}(\mathbf{k}^r, \mathbf{k}^r) = \frac{k_m}{4\pi i} (\overleftrightarrow{\mathbf{I}} - \hat{\mathbf{k}}^r \hat{\mathbf{k}}^r) \cdot \overleftrightarrow{\mathbf{T}}(\mathbf{k}^r, \mathbf{k}^r) \cdot \hat{\mathbf{e}}_r = S(0) \hat{\mathbf{e}}_r, \quad (43b)$$

$$\mathbf{S}(\mathbf{k}^r, \mathbf{k}^i) = \frac{k_m}{4\pi i} (\overleftrightarrow{\mathbf{I}} - \hat{\mathbf{k}}^r \hat{\mathbf{k}}^r) \cdot \overleftrightarrow{\mathbf{T}}(\mathbf{k}^r, \mathbf{k}^i) \cdot \hat{\mathbf{e}}_i = S_j(\pi - 2\theta_i) \hat{\mathbf{e}}_r, \quad (43c)$$

$$\mathbf{S}(\mathbf{k}^i, \mathbf{k}^r) = \frac{k_m}{4\pi i} (\overleftrightarrow{\mathbf{I}} - \hat{\mathbf{k}}^i \hat{\mathbf{k}}^i) \cdot \overleftrightarrow{\mathbf{T}}(\mathbf{k}^i, \mathbf{k}^r) \cdot \hat{\mathbf{e}}_r = S_j(\pi - 2\theta_i) \hat{\mathbf{e}}_i. \quad (43d)$$

where $\hat{\mathbf{e}}_r$ is the polarization vector of a specularly reflected wave, $S(0)$ is the forward scattering amplitude of an isolated sphere (embedded in the matrix medium), the subindex j takes the value 1 for a TE incident polarized wave (s polarization) and 2 for a TM polarized wave (p polarization) and S_1 and S_2 are the diagonal elements of the amplitude scattering matrix of an isolated sphere (also embedded in the matrix medium) as defined by Bohren and Huffman in [37]. The first and third of these identities were previously established in [18,19] and the other two are demonstrated in the same way. It is immediate to see that the polarization vectors $\hat{\mathbf{e}}_i$ and $\hat{\mathbf{e}}_r$ in the present geometry are given by $\hat{\mathbf{e}}_i = \hat{\mathbf{a}}_x$ and $\hat{\mathbf{e}}_r = \hat{\mathbf{a}}_x$ for a TE polarized incident wave and by $\hat{\mathbf{e}}_i = \cos \theta_i \hat{\mathbf{a}}_y - \sin \theta_i \hat{\mathbf{a}}_z$ and $\hat{\mathbf{e}}_r = \cos \theta_i \hat{\mathbf{a}}_y + \sin \theta_i \hat{\mathbf{a}}_z$ for a TM polarized incident wave.

With the above identities the coherent reflection and transmission coefficients are given by

$$r_{\text{coh}} = \frac{-\alpha S_j(\pi - 2\theta_i)}{1 + \alpha S(0) + \frac{\alpha^2}{4} (S^2(0) - S_j^2(\pi - 2\theta_i))}, \quad (44a)$$

and

$$t_{\text{coh}} = \left(\frac{1 - \frac{\alpha^2}{4} (S^2(0) - S_j^2(\pi - 2\theta_i))}{1 + \alpha S(0) + \frac{\alpha^2}{4} (S^2(0) - S_j^2(\pi - 2\theta_i))} \right), \quad (44b)$$

where, as already mentioned, $j = 1$ or 2 for a TE or a TM polarized incident wave, respectively. If we drop the second-order terms in α , we recover the corresponding expressions obtained previously in [29], that is,

$$t_{\text{coh}} = \frac{1}{1 + \alpha S(0)}, \quad (45a)$$

and

$$r_{\text{coh}} = \frac{\alpha S_j(\pi - 2\theta_i)}{1 + \alpha S(0)}. \quad (45b)$$

Let us recall that in [29] the coefficients given in Eqs. (45a) and (45b) were obtained heuristically by simply assuming that the exciting field is equal to the transmitted field. From the multiple-scattering treatment presented here we can see now that the exciting field is actually composed by a transmitted component and a reflected one.

It is not difficult to see that, if we were only to take the SS, the transmission and reflection coefficients of the monolayer would be given by, $t_{\text{coh}}^{\text{SS}} = 1 - \alpha S(0)$ and $r_{\text{coh}}^{\text{SS}} = \alpha S_j(\pi - 2\theta_i)$. Clearly in these expressions, the magnitude of the

single-scattering coefficients grow without bound whenever the angle of incidence approaches grazing, because the expression for α has the cosine of the angle of incidence in the denominator [see Eq. (38)]. Nevertheless, for sufficiently small angles of incidence and sufficiently small surface coverage the SS can be accurate and we will use it below in the numerical examples for comparison purposes.

E. Accuracy of the Model Predictions

The results in Eqs. (44a) and (44b) were obtained assuming a hard-sphere pair-correlation function and neglecting the contributions from the side strips on the integrals over d^3r^n . If we were willing and proficient enough to improve any of these approximations other terms of second-order and higher on the surface density of particles, ρ_s , will be added on the numerator and on the denominator of the expressions in Eqs. (44a) and (44b). Therefore, whenever the contribution of the second-order terms in ρ_s appearing in Eqs. (44a) and (44b) is small, the predictions of the models should be accurate. This means that when the coherent reflection and transmission coefficients predicted by Eqs. (44a) and (44b) and by (45a) and (45b) are numerically close to each other, the HM and multiple-scattering models (MSM) should both be accurate. When the two approximations differ, we should deem the predictions from Eqs. (44a) and (44b) better, but we should start being cautious about it accuracy. As it turns out, this criterion gives an ample range in the parameters of a monolayer where we can use confidently the present model. However, it will be necessary to compare with numerical solutions to the problem and experimental data to delineate the regions of validity of the MSM for monolayers with higher surface coverage.

4. MONOLAYER SUPPORTED BY A FLAT INTERFACE

If we now assume that the monolayer is supported by a flat interface, we must take into account the multiple reflections of the average wave between the monolayer and the flat interface. Let us assume that light is incident at an angle θ_1 to a flat interface between medium 1 and 2 with refractive indices n_1 and n_2 , as shown in Fig. 3. We can construct the coherent reflection coefficient by replacing the monolayer with an effective infinitely thin layer with a reflection and transmission coefficient given by Eqs. (44a) and (44b), respectively. If the particles are adsorbed on the interface, this effective, infinitely thin layer is parallel to the interface and one particles radius apart. Now, if the particles sit on the interface from the incidence side, we have that the matrix medium for the monolayer is medium 1 and $n_m = n_1$. If the particles are adsorbed to the interface from the external medium, the matrix is medium 2 and $n_m = n_2$. The angle of incidence of light to the monolayer is $\theta_i = \theta_1$ when the particles are on the side of medium 1. However, when the particles are below the interface, that is, immersed in medium 2, light gets refracted before reaching the monolayer and thus, the angle of incidence to the particles is given by Snell's law as $\theta_2 = \sin^{-1}[(n_1/n_2) \sin \theta_1]$.

In the case when the particles sit on the interface on the side of the incidence medium, the multiple reflections of the coherent wave between the monolayer plane and the interface is given by

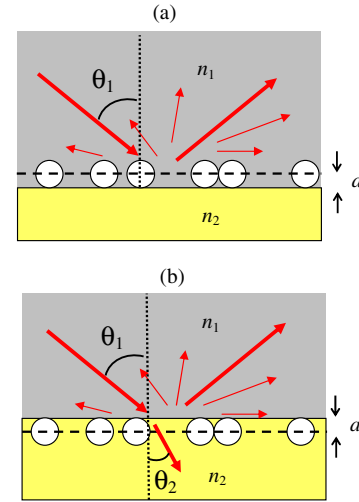


Fig. 3. (Color online) Illustration of the monolayer supported by a flat interface. (a) The particles are sitting on the interface and embedded in medium 1 and (b) the particles are below the interface in medium 2. Note that, in (b) the angle of incidence to the monolayer plane is θ_2 and is related to θ_1 by Snell's law between medium 1 and medium 2. In both cases the plane of the monolayer is indicated by the dashed line parallel to the interface and separated by one particle's radius (a).

$$r = r_{\text{coh}}(\theta_1) + r_{12}(\theta_1)t_{\text{coh}}^2(\theta_1)\exp(\beta_1) + r_{\text{coh}}(\theta_1)r_{12}^2(\theta_1)t_{\text{coh}}^2(\theta_1)\exp(2\beta_1) + r_{\text{coh}}^2(\theta_1)r_{12}^3(\theta_1)t_{\text{coh}}^2(\theta_1)\exp(3\beta_1) + \dots,$$

where $\beta_1 = 2ik_0an_1 \cos \theta_1$ and r_{12} is the Fresnel reflection coefficient of the interface between refractive indices, n_1 and n_2 evaluated at an angle of incidence θ_1 . This sum is simplified to

$$r(\theta_1) = r_{\text{coh}}(\theta_1) + \frac{r_{12}(\theta_1)t_{\text{coh}}^2(\theta_1)\exp(\beta_1)}{1 - r_{12}(\theta_1)r_{\text{coh}}(\theta_1)\exp(\beta_1)}, \quad (47)$$

where r_{coh} and t_{coh} are the coherent reflection and transmission coefficients of the free-standing monolayer with particles embedded in medium 1.

Now, when the particles are behind the interface inside medium 2, we get

$$r = r_{12}(\theta_1) + t_{12}(\theta_1)t_{21}(\theta_2)r_{\text{coh}}(\theta_2)\exp(\beta_2)[1 + r_{\text{coh}}(\theta_2)r_{21}(\theta_2)\exp(\beta_2) + (r_{\text{coh}}(\theta_2)r_{21}(\theta_2))^2\exp(2\beta_2) + \dots]$$

where $\beta_2 = 2ik_0an_2 \cos \theta_2$. Noting that, $t_{12}(\theta_1) = 1 + r_{12}(\theta_1)$, $t_{21}(\theta_2) = 1 + r_{21}(\theta_2)$, and $r_{21}(\theta_2) = -r_{12}(\theta_1)$ we can simplify the sum as

$$r(\theta_1) = \frac{r_{12}(\theta_1) + r_{\text{coh}}(\theta_2)\exp(\beta_2)}{1 + r_{12}(\theta_1)r_{\text{coh}}(\theta_2)\exp(\beta_2)}, \quad (48)$$

where r_{coh} is the coherent reflection coefficients of the free-standing monolayer with particles embedded in medium 2 and as already said, $\theta_2 = \sin^{-1}[(n_1/n_2) \sin \theta_1]$.

5. NUMERICAL EXAMPLES

Let us now evaluate the reflection and transmission coefficients in Eqs. (44a) and (44b) for a few examples, and refer to these coefficients as the ones of the MSM. For comparison purposes we will refer to the coefficients in Eqs. (45a) and (45b) as the ones of the HM and to $r_{\text{coh}}^{\text{SS}} = 1 - \alpha S(0)$ and $r_{\text{coh}}^{\text{SS}} = \alpha S_j(\pi - 2\theta_i)$ as the ones where the SS has been used. Introducing now these coefficients in either Eq. (47) or (48), gives the MSM, HM, or SS reflection coefficients of a monolayer supported by a flat interface.

In Figs. 4–6 we plot the coherent reflectance and transmittance of a linearly polarized incident plane wave from a free-standing monolayer of particles immersed in air ($n_m = 1.0$) varying one of the optical parameter's of the particles. The surface coverage is assumed to be moderately small.

In Fig. 4 we assume relatively large particles of size parameter 10 and vary the real part of the particles' refractive index assuming the imaginary part is zero. Note that the coherent reflectance in this example is very small and does not compensate the large drop in coherent transmittance as the refractive index (assumed real) increases. In this example the energy flux missing in the coherently reflected transmitted fields is all transformed to energy flux in the diffuse field since in this example the particles do not absorb light.

In Fig. 5 we assume the same large particles of size parameter 10 but with a complex refractive index with its real part fixed at 1.3 and we vary its imaginary part from 0 to 1 and thus adding optical absorption to the particles. The first points in these graphs correspond to those for a refractive index of 1.3 in Fig. 4. We can see in Fig. 5 that the coherent transmittance predicted by the three models is rather insensitive (in relative terms) to $\text{Im}(n_p)$, whereas the coherent reflectance does change appreciably in relative terms as $\text{Im}(n_p)$ increases. From only the coherent transmittance and reflectance calculated here we cannot tell how much light is missing from the coherent fields goes into the diffuse field and how much gets actually absorbed by the particles. It would be necessary to calculate the diffusely reflected and transmitted fields.

In Fig. 6 we consider highly absorbing particles and vary their radius from infinitesimally small to relatively large particles of size parameter about 2.5. We can appreciate in these figures that the reflectance predicted by the MSM and the HM remain close to each other, whereas the transmittance differs noticeably. In all cases shown in the figure, the SS deviates strongly either from the MSM or the HM or from both. In Fig. 5b and 6b the reflectance or transmittance calculated by the SS reaches values larger than 1, which is of course, a nonphysical result.

In Figs. 7 and 8 we plot a spectrum of the coherent reflectance of a free-standing and a supported monolayer, respectively, of gold particles of 50 nm radius and a surface-coverage of 0.25. We assume normally incident and obliquely incident light at 60° for both polarizations TE and TM. The peak in reflectance seen around a wavelength of 500 nm is due to the so called surface plasmon resonance of the particles. For ease of comparison of both figures, the dielectric supporting the monolayer assumed in Fig. 8 was supposed to be dispersionless with a refractive index of 1.5 for all wavelengths. It is interesting to note that the effect of the substrate is to lower the reflectance of the monolayer of gold particles. The height of

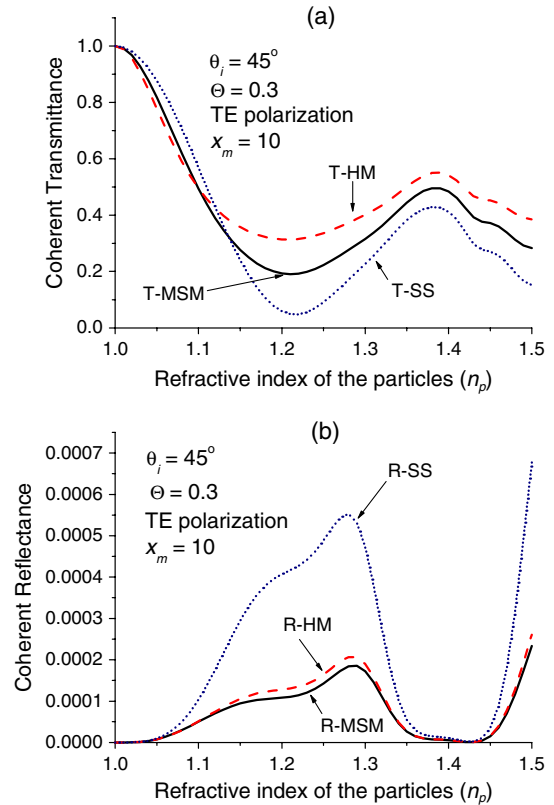


Fig. 4. (Color online) Plot of the coherent (a) transmittance and (b) reflectance of a free-standing monolayer of particles of size parameter $x_m = 10$ immersed on air ($n_m = 1.0$) as a function of the particle refractive index (assumed real). The angle of incidence is $\theta_i = 45^\circ$, surface-coverage-fraction is $\Theta = 0.3$, and the polarization of light is assumed TE. The solid line (black on line) is for the multiple-scattering model (MSM), the dashed line (red on line) is for the heuristic model (HM), and the short dash (navy on line) is for the single-scattering model (SS).

the peak in absorption is clearly smaller when the monolayer is supported than if it is free standing. In these plots the HM and the MSM are close to each other throughout the range in wavelengths shown in the plots, whereas the SS approximation clearly overestimates the reflectance from the monolayer throughout the visible range and part of the near infrared portions of the spectrum.

In Fig. 9 we plot the spectrum of the coherent reflectance from a monolayer of silver particles sitting on top of silver with a surface-coverage of 0.25. We assumed light is incident at 30° and plot the results for both polarizations TE and TM. In this example the single SS approximation fails drastically predicting a reflectance larger than 1 for most wavelengths in the graph. We can see the HM and the MSM results differ from each other, more for TM than for TE polarized light. In Fig. 8(a) we can appreciate that the HM reaches values slightly above 1 at the largest wavelengths shown in the graph whereas the MSM remains below 1. It is interesting to see that the monolayer of silver particles strongly reduces the reflectivity of the silver interface in the blue portion of the spectrum but it reduces it only slightly in the deep red and near infrared portions of the spectrum.

For both, gold and silver particles, assumed in Figs. 6, 7, and 8, respectively, we assumed the refractive index of the particles equal to that of the bulk metal.

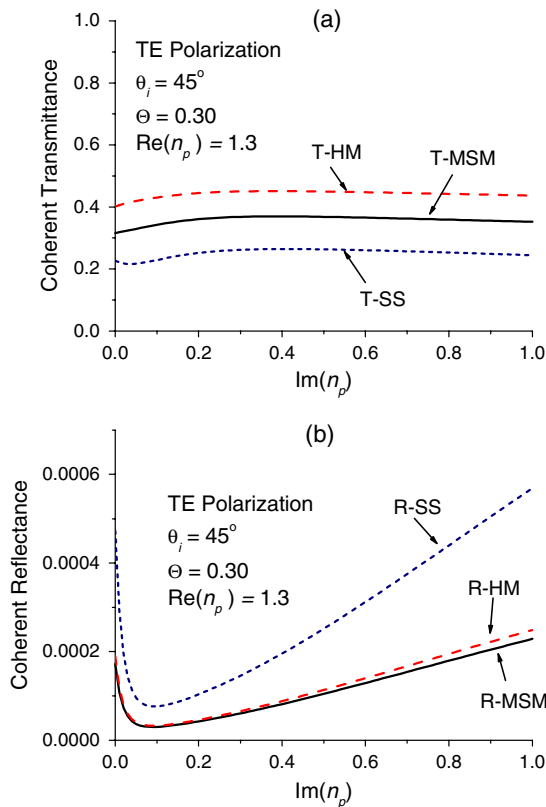


Fig. 5. (Color online) Plot of the coherent (a) transmittance and (b) reflectance of a free-standing monolayer of particles of size parameter $x_m = 10$ and a refractive index with its real part, $\text{Re}(n_p)$, equal to 1.3, immersed on air ($n_m = 1.0$) as a function of the imaginary part of the particle refractive index. The angle of incidence is $\theta_i = 45^\circ$, surface-coverage-fraction is $\Theta = 0.3$, and the polarization of light is assumed TE. The solid line (black on line) is for the multiple-scattering model (MSM), the dashed line (red on line) is for the heuristic model (HM) and the short dash (navy on line) is for the single-scattering model (SS).

Finally, in Fig. 10 we plot the reflectance of TM polarized light versus the angle of incidence from a glass-water interface with a monolayer of Polystyrene particles ($n_p = 1.59$) adsorbed from the water side and light incident from the glass side (internal reflection). Relatively large particles are used with radii of 100, 200, and 300 nm. The wavelength of light in vacuum used in the calculations is 635 nm. In this case, in the absence of the monolayer there is a critical angle near

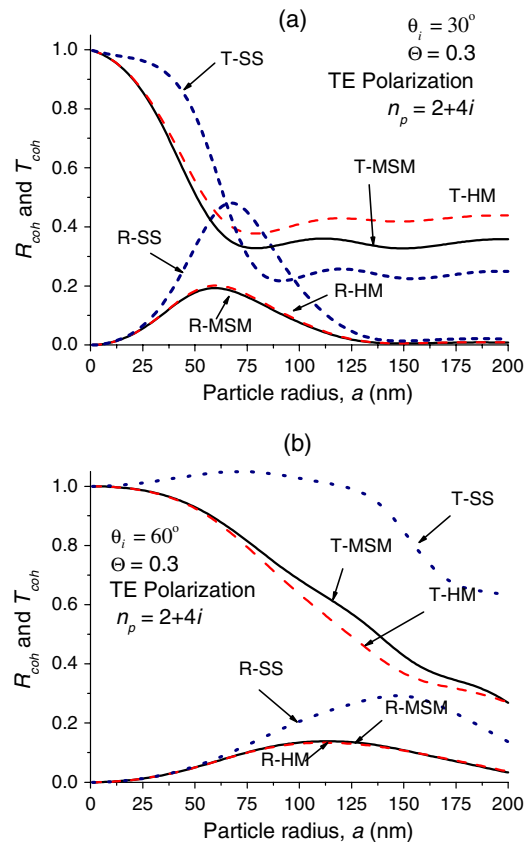


Fig. 6. (Color online) Plot of the coherent reflectance and transmittance of a free-standing monolayer of particles in air ($n_m = 1.0$) as a function of the particle radius at two different angles of incidence (a) $\theta_i = 30^\circ$ and (b) $\theta_i = 60^\circ$ at a fixed surface-coverage-fraction $\Theta = 0.3$. The refractive index of the particles is $n_p = 2+4i$, the wavelength of radiation is assumed to be $\lambda = 500$ nm and the polarization of light is TE. The solid line (black on line) is for the multiple-scattering model (MSM), the dashed line (red on line) is for the heuristic model (HM) and the short dash (navy on line) is for the single-scattering model (SS).

62° and behind it we have total internal reflection. Clearly the presence of a monolayer of particles adsorbed on the surface frustrates the total internal reflection through scattering and absorption of the coherent wave. We can see in Fig. 10(a) that the MSM and HM remain very close to each other for all angles of incidence for the smaller particles, but important differences are seen in Figs. 10(b) and 10(c) for particles of 200

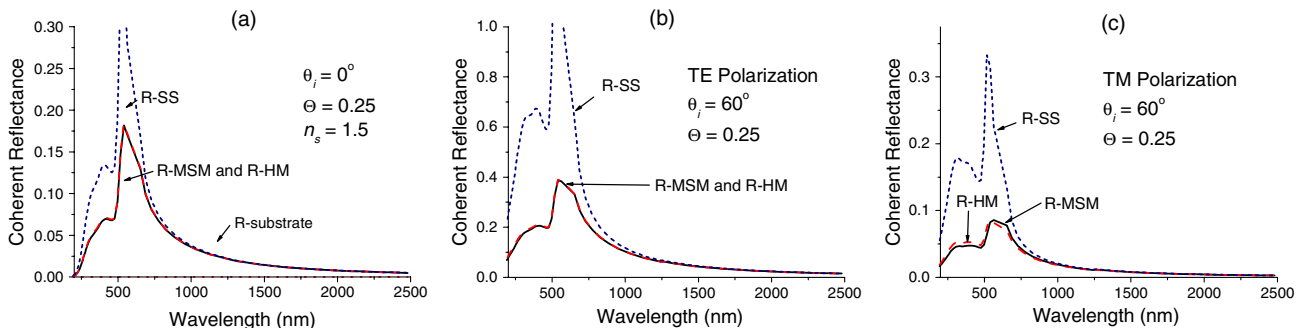


Fig. 7. (Color online) Calculated spectra of the coherent reflectance of a free-standing monolayer of gold particles in air. (a) For an angle of incidence of $\theta_i = 0^\circ$, (b) For an angle of incidence of $\theta_i = 60^\circ$ and TE polarization, (c) For an angle of incidence of $\theta_i = 0^\circ$ and TM polarization. The particle radius is $a = 50$ nm and the surface-coverage-fraction is $\Theta = 0.25$. The solid line (black on line) is for the multiple-scattering model (MSM), the dashed line (red on line) is for the heuristic model (HM) and the short dash (navy on line) is for the single-scattering model (SS).

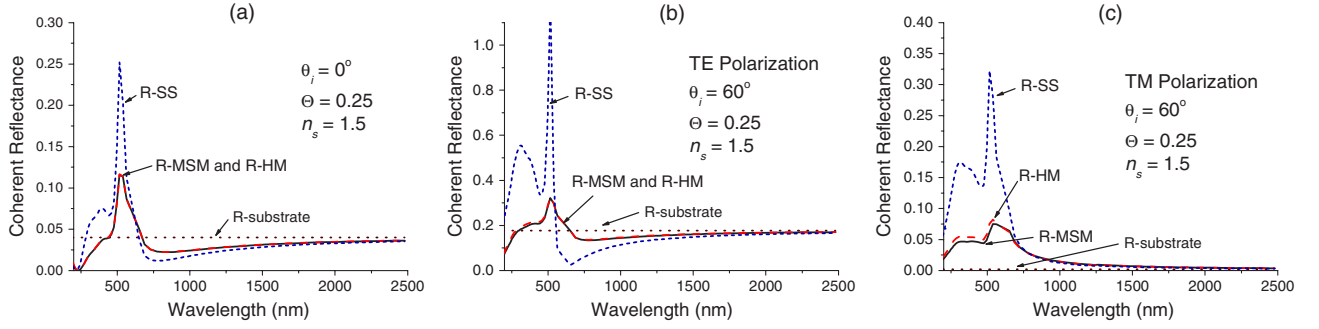


Fig. 8. (Color online) Calculated spectra of the coherent reflectance of a monolayer of gold particles sitting on top of an air-glass interface ($n_m = 1.0$ and $n_s = 1.5$) (a) for an angle of incidence of $\theta_i = 0^\circ$, (b) for an angle of incidence of $\theta_i = 60^\circ$ and TE polarization, (c) for an angle of incidence of $\theta_i = 60^\circ$ and TM polarization. The particle radius is $a = 50$ nm and the surface-coverage fraction is $\Theta = 0.25$. The reflectance of the substrate alone (without the monolayer) is the dotted line (brown on line), the solid line (black on line) is for the multiple-scattering model (MSM), the dashed line (red on line) is for the heuristic model (HM) and the short dash (navy on line) is for the single-scattering (SS).

and 300 nm radius for angles of incidence larger than the critical angle. In this example the wave incident to the monolayer is an evanescent wave decaying along the z -axis when the angle of incidence is larger than the critical angle for the glass-water interface. This evanescent wave is actually an incident plane wave with a complex angle of incidence. There is no

additional difficulty in evaluating the amplitude scattering functions S_1 and S_2 with a complex angle of incidence using the standard algorithms from Mie theory [37].

From the examples in Figs. 4–10, we can get a rough idea of the validity of the MSM and HM. We can see that there is wide range of particle radius and refractive indices for which the MSM can be used with confidence.

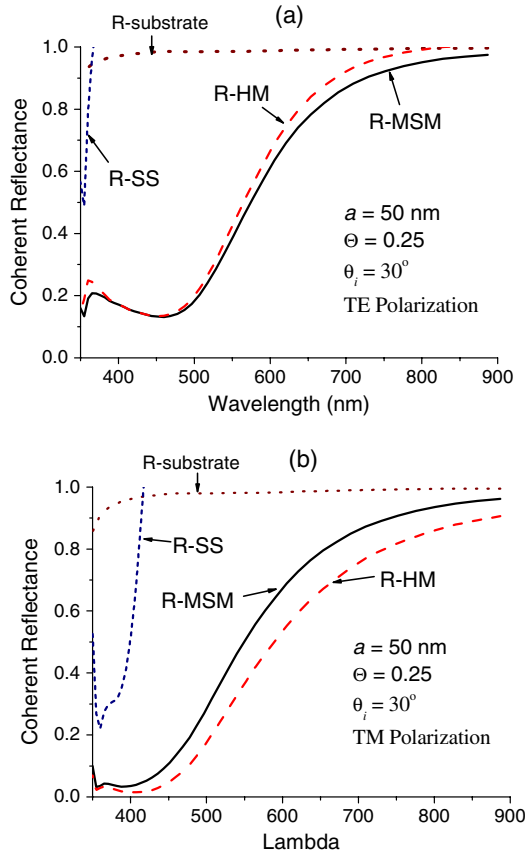


Fig. 9. (Color online) Calculated spectra of the coherent reflectance of a monolayer of silver particles sitting on top of silver half-space ($n_m = 1.0$ and $n_s(\omega)$ is that of silver). The particle radius is $a = 50$ nm, the angle of incidence is $\theta_i = 30^\circ$, the surface-coverage fraction $\Theta = 0.25$ and the polarization is (a) TE and (b) TM. The reflectance of the substrate alone (without the monolayer) is the dotted line (brown on line), the solid line (black on line) is for the multiple-scattering model (MSM), the dashed line (red on line) is for the heuristic model (HM), and the short dash (navy on line) is for the single-scattering model (SS).

6. FINAL REMARKS

Upon using the MSM it may help to note that the second-order term ($\alpha^2/4)(S^2(0) - S_j^2(\pi - 2\theta_i))$ that appears in Eqs. (44a) and (44b), with j either 1 or 2, does not diverge as the angle of incidence approaches grazing. This can be readily seen by expanding $S_j(\pi - 2\theta_i)$ in powers of the difference between the angle of incidence and $\pi/2$. We have, $S_j(\pi - 2\theta_i) \approx S_j(0) + \frac{1}{2}[S_j''(0)]4(\delta\theta)^2 + O(\delta\theta)^3$, where $\delta\theta \equiv \pi/2 - \theta_i$ and $S_j''(0)$ is the second derivative of S_j with respect to its argument evaluated in the forward direction. The first-order term is zero since the scattering amplitude is maximum in the forward direction and thus, $S_j'(0) = 0$. On the other hand the parameter $\alpha = 2\Theta/x_m^2 \cos(\pi/2 - \delta\theta) \approx 2\Theta/(x_m^2 \delta\theta)$. Thus, in the limit of grazing incidence we have

$$\frac{\alpha^2}{4}(S^2(0) - S_j^2(\pi - 2\theta_i)) \rightarrow -4 \frac{\Theta^2}{x_m^4} S(0)S_j''(0), \quad (49)$$

which is a finite number since $S_j''(0)$ is finite.

An interesting limit, for future reference, is the small particle limit of the coherent reflection and transmission coefficients obtained above. These are readily obtained using the following results given in [37], $S_1(\pi - 2\theta_i) \rightarrow S(0) \rightarrow -ix_m^3\chi$ and $S_2(\pi - 2\theta_i) \rightarrow -ix_m^3\chi \cos(\pi - 2\theta_i)$, where $\chi \equiv (n_p^2 - n_m^2)/(n_p^2 + 2n_m^2)$. Then, for TE polarization in the limit of small particles the reflection and transmission coefficients tend, for TE polarization to

$$r_{\text{coh}}^{\text{TE}} \rightarrow \frac{i\beta\chi}{1 - i\beta\chi}, \quad t_{\text{coh}}^{\text{TE}} \rightarrow \frac{1}{1 - i\beta\chi}, \quad (50a)$$

and for TM polarization to

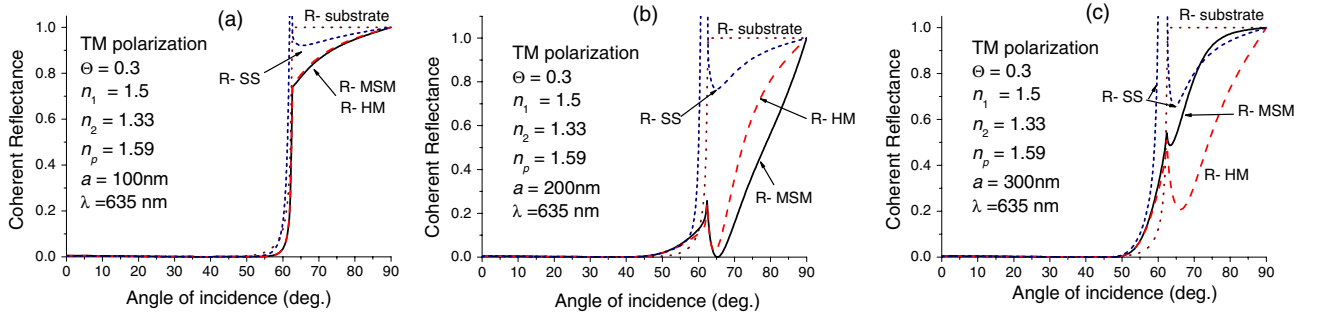


Fig. 10. (Color online) Plot of the coherent reflectance of a monolayer of particles adsorbed below a glass–water interface (from the water’s side) ($n_1 = 1.5$, $n_2 = 1.33$, $n_m = 1.33$) as a function of the angle of incidence. The particle refractive index is $n_p = 1.59$ (e.g. polystyrene) and the particle radius is (a) $a = 100$ nm, (b) $a = 200$ nm, and (c) $a = 300$ nm. The wavelength in vacuum of the light is $\lambda = 635$ nm. The polarization of light is TM. The reflectance of the substrate alone (without the monolayer) is the dotted line (brown on line), the solid line (black on line) is for the multiple-scattering model (MSM), the dashed line (red on line) is for the heuristic model (HM), and the short dash (navy on line) is for the single-scattering model (SS).

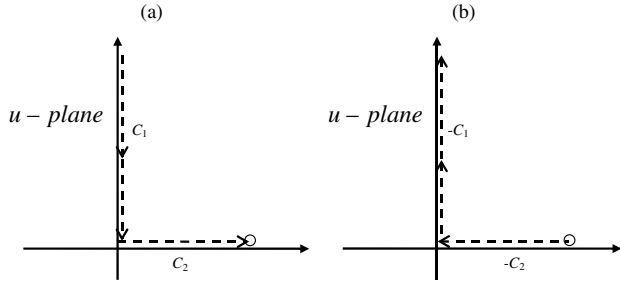


Fig. 11. (a) First half and (b) second half of the path of integration in Eq. (B1) in the complex u –plane. The open circle indicates schematically where $u = k_m$ and the function $k_z^s = [k_m^2 - u^2]^{1/2}$ has a branch point.

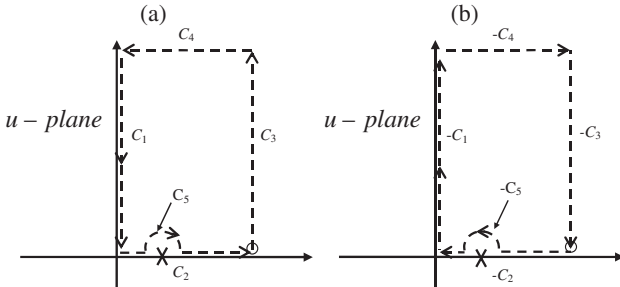


Fig. 12. Closed contours used to evaluate the principal value of the integrals on (a) Γ_1 and (b) Γ_2 in Eq. (B2). The open circle indicates schematically where $u = k_m$ and the function $k_z^s = [k_m^2 - u^2]^{1/2}$ has a branch point.

$$r_{\text{coh}}^{\text{TM}} \rightarrow \frac{i\beta\chi \cos(\pi - 2\theta_i)}{1 - i\beta\chi - \frac{1}{4}\beta^2\chi^2 \sin^2(\pi - 2\theta_i)},$$

$$t_{\text{coh}}^{\text{TM}} \rightarrow \frac{1 + \frac{1}{4}\beta^2\chi^2 \sin^2(\pi - 2\theta_i)}{1 - i\beta\chi - \frac{1}{4}\beta^2\chi^2 \sin^2(\pi - 2\theta_i)}, \quad (50b)$$

where $\beta = 2\Theta x_m / \cos \theta_i$. The small particle limit for the HM is obtained from the latter expressions dropping the second-order terms $\beta\chi$ in the numerator or denominator. Note that the second-order term appearing in Eqs. (50a) and (50b), $\beta^2\chi^2 \sin^2(\pi - 2\theta_i)$ give a finite contribution in the limit $\theta_i \rightarrow \pi/2$, as previously said. For the SS we expand the denominators in powers of $\beta\chi$ and keep terms to first-order only. It is interesting to point out a fundamental flaw of the SS: The transmission coefficients for both polarizations in the small

particle limit is $t_{\text{coh}}^{\text{SS}} = 1 + i\beta\chi$ and thus, the transmittance in this limit $|t_{\text{coh}}^{\text{SS}}|^2 = 1 + \beta^2|\chi|^2 - 2\beta\text{Im}(\chi)$, which give values larger than 1 for any angle of incidence if χ is real or if it has a small imaginary part such that $\text{Im}(\chi) < \frac{1}{2}\beta|\chi|^2$. This is true even for very low surface coverage. Actually this unphysical feature of the SS was clearly pointed out before in [26]. It can be appreciated here in Fig. 6(b). This flaw is not present neither in the HM nor the MSM. It is clear that being $|t_{\text{coh}}^{\text{SS}}|^2$ a second-order expression in $\beta\chi$ when the particles have a real refractive index, this flaw comes from neglecting all second-order terms.

7. SUMMARY AND CONCLUSIONS

Using a multiple-scattering formalism we derived relatively simple closed-form expressions for the coherent reflection and transmission coefficients of light from a random monolayer of particles of arbitrary size. We considered only spherical particles made of an isotropic material embedded in a transparent isotropic and homogeneous medium. The expressions are derived within the so called QCA which provides us with an integral equation for the electric field exciting the particles. We assumed the two-particle correlation function is a simple correlation hole, which is a valid approximation only for moderately small surface-coverage fractions. We assumed an Ansatz for the exciting fields in the form of an effective plane wave traveling in the direction of incidence plus another effective plane wave traveling in the direction of coherent reflection (the specular direction). Introducing the Ansatz in the QCA equation for the average exciting electric fields, performing the required integrals and keeping only the leading terms that produce effective plane waves traveling in the incidence and specular directions, yield two consistency equations from which the complex amplitudes and polarization of the effective plane-waves contained in the Ansatz are determined. Once having the desired approximation to the effective exciting fields, we calculate the average of the scattered fields at either side of the monolayer and determine the reflection and transmission coefficients for the average or coherent wave.

The latter approximations limit the validity of the model to moderately small surface-coverage fractions, allowing, however, for any particle size and angle of incidence. By dropping second-order terms in the numerator and in the denominator of the derived expressions for r_{coh} and t_{coh} we obtain the expressions derived in our previous model which we refer to as

the HM. We deem the differences between the predictions of the multiple-scattering and HMs as a confidence gauge for the MSM. Numerical examples using both models suggest the MSM just derived has a wide range of validity in problems already of interest in many applications. We also compared with the SS and found that this simpler approximation is severely limited in validity and in our opinion it is more strongly limited than what is commonly accepted. The effect of a substrate supporting the monolayer was also introduced using a simple approach of taking into account the multiple reflections of the coherent wave between the monolayer and the substrate.

Further analysis is necessary to delineate the limits of applicability of the MSM obtained here and should be dealt with in prospect works. Nevertheless, we believe the model can be readily applied to a wide variety of interesting problems with assurance to a good extent accordingly to the confidence gauge discussed above.

APPENDIX A

The contribution to the QCA equation coming from integrating on dr_n^3 on the strip where $|y_j - y_n| < 2a$ can be split in two (again, see Fig. 2). To simplify, let us assume the exclusion area as a square of sides $4a$. Then the contribution from the left semistrip (Lss) corresponds to integrating in x_n from $-\infty$ to $x_j - 2a$ and the contribution from the right semistrip (Rss) corresponds to integrating from $x_j + 2a$ to ∞ . That is,

$$\begin{aligned} \int_{\text{Lss}} d^3r_n(\cdot) &\rightarrow \int_0^{\Delta z} \int_{y_j-2a}^{y_j+2a} \int_{-L}^{x_j-2a} dx_n dy_n dz_n(\cdot), \\ \int_{\text{Rss}} d^3r_n(\cdot) &\rightarrow \int_0^{\Delta z} \int_{y_j-2a}^{y_j+2a} \int_{x_j+2a}^L dx_n dy_n dz_n(\cdot). \end{aligned}$$

The appropriate expansion of the dyadic Green's function for the integrals over these semistrips is

$$\begin{aligned} \vec{\mathbf{G}}(\mathbf{r}, \mathbf{r}') &= -\hat{\mathbf{a}}_x \hat{\mathbf{a}}_x \delta(\mathbf{r} - \mathbf{r}') + \frac{i}{2} \iint \frac{dk_y^s dk_z^s}{(2\pi)^2} \frac{1}{k_x^s} (\vec{\mathbf{I}} - \hat{\mathbf{k}}_{\pm}^s \hat{\mathbf{k}}_{\pm}^s) \\ &\cdot \exp[i\mathbf{k}_{\pm}^s \cdot (\mathbf{r} - \mathbf{r}')], \end{aligned} \quad (\text{A1})$$

with $\mathbf{k}_{\pm}^s = \pm k_x^s \hat{\mathbf{a}}_x + k_y^s \hat{\mathbf{a}}_y + k_z^s \hat{\mathbf{a}}_z$ and $k_x^s = \sqrt{k_m^2 - (k_y^s)^2 - (k_z^s)^2}$. For an exciting field of the form, $\mathbf{E}_p^{\text{exc}}(\mathbf{r}) = E_{\text{exc}} \exp(i\mathbf{k}_D \cdot \mathbf{r}_p) \exp(i\mathbf{k}^{\text{exc}} \cdot \mathbf{r}) \hat{\mathbf{e}}_{\text{exc}}$ with $\mathbf{k}^{\text{exc}} = k_y^{\text{exc}} \hat{\mathbf{a}}_y + k_z^{\text{exc}} \hat{\mathbf{a}}_z$ and $\mathbf{k}_D = \mathbf{k}_{\parallel}^i - \mathbf{k}^{\text{exc}}$, the induced field due to the integral over d^3r_n over the left semistrip (in which x is always larger than x' whenever the integrand is not zero) is

$$\begin{aligned} \mathbf{E}_{\text{Lss}}^{\text{ind}}(\mathbf{r}) &= \frac{i\rho_s}{2} E_{\text{exc}} \iint \frac{dk_y^s dk_z^s}{(2\pi)^2} \frac{1}{k_x^s} (\vec{\mathbf{I}} - \hat{\mathbf{k}}_{+}^s \hat{\mathbf{k}}_{+}^s) \cdot \vec{\mathbf{T}}(\mathbf{k}_{+}^s, \mathbf{k}^{\text{exc}}) \cdot \hat{\mathbf{e}}_{\text{exc}} \\ &\times \left(\frac{\exp[-ik_x^s(x_j - 2a)] - \exp(ik_x^s L)}{-ik_x^s} \right) \\ &\times \left(\frac{2i \sin[(k_y^i - k_y^s)2a]}{i(k_y^i - k_y^s)} \right) \\ &\times \exp[i(k_y^i - k_y^s)y_j] \exp[i\mathbf{k}_{+}^s \cdot \mathbf{r}], \end{aligned} \quad (\text{A2})$$

where $\mathbf{k}_{+}^s = k_x^s \hat{\mathbf{a}}_x + k_y^s \hat{\mathbf{a}}_y + k_z^s \hat{\mathbf{a}}_z$ with $k_x^s = \sqrt{k_m^2 - (k_y^s)^2 - (k_z^s)^2}$. To see whether this field contributes appreciably in comparison with the fields induced by the particles in the bottom half-plane of the monolayer we must compare Eq. (A2) with the corresponding expression for $\mathbf{E}_B^{\text{ind}}$,

$$\begin{aligned} \mathbf{E}_B^{\text{ind}}(\mathbf{r}, \mathbf{r}_j) &= \frac{i\rho_s}{2} E_{\text{exc}} \iint \frac{dk_x^s dk_z^s}{(2\pi)^2} \frac{1}{k_y^s} (\vec{\mathbf{I}} - \hat{\mathbf{k}}_{+}^s \hat{\mathbf{k}}_{+}^s) \cdot \vec{\mathbf{T}}(\mathbf{k}_{+}^s, \mathbf{k}^{\text{exc}}) \\ &\cdot \hat{\mathbf{e}}_{\text{exc}} \exp[i\mathbf{k}_{+}^s \cdot \mathbf{r}] \times \left[\frac{2i \sin(k_x^s L)}{ik_x^s} \right] \\ &\times \left[\frac{\exp[i(k_y^i - k_y^s)(y_j - 2a)] - \exp[-i(k_y^i - k_y^s)L]}{i(k_y^i - k_y^s)} \right]. \end{aligned} \quad (\text{A3})$$

For ease of comparison let us change the integration variables in both expressions to a polar coordinate system. We do

$$\iint dk_y^s dk_z^s \rightarrow \int_0^{2\pi} \int_0^{\infty} d\theta \rho d\rho, \quad \iint dk_x^s dk_z^s \rightarrow \int_0^{2\pi} \int_0^{\infty} d\theta \rho d\rho,$$

in Eq. (A2) and Eq. (A3), respectively. Then we get

$$\begin{aligned} \mathbf{E}_{\text{Lss}}^{\text{ind}}(\mathbf{r}) &= \frac{i\rho_s}{2} E_{\text{exc}} \int_0^{2\pi} \int_0^{\infty} \frac{d\theta \rho d\rho}{(2\pi)^2} \frac{1}{\sqrt{k_m^2 - \rho^2}} (\vec{\mathbf{I}} - \hat{\mathbf{k}}_{+}^s \hat{\mathbf{k}}_{+}^s) \\ &\cdot \vec{\mathbf{T}}(\mathbf{k}_{+}^s, \mathbf{k}^{\text{exc}}) \cdot \hat{\mathbf{e}}_{\text{exc}} \exp[i\mathbf{k}_{+}^s \cdot \mathbf{r}] \\ &\times \left(\frac{\exp[-i\sqrt{k_m^2 - \rho^2}(x_j - 2a)] - \exp[i\sqrt{k_m^2 - \rho^2}L]}{-i\sqrt{k_m^2 - \rho^2}} \right) \\ &\times \left(\frac{2i \sin[(k_y^i - \rho \sin \theta)2a]}{i(k_y^i - \rho \sin \theta)} \right) \exp[i(k_y^i - \rho \sin \theta)y_j], \end{aligned} \quad (\text{A4})$$

and

$$\begin{aligned} \mathbf{E}_B^{\text{ind}}(\mathbf{r}, \mathbf{r}_j) &= \frac{i\rho_s}{2} E_{\text{exc}} \int_0^{2\pi} \int_0^{\infty} \frac{d\theta \rho d\rho}{(2\pi)^2} \frac{1}{\sqrt{k_m^2 - \rho^2}} (\vec{\mathbf{I}} - \hat{\mathbf{k}}_{+}^s \hat{\mathbf{k}}_{+}^s) \cdot \vec{\mathbf{T}}(\mathbf{k}_{+}^s, \mathbf{k}^{\text{exc}}) \cdot \hat{\mathbf{e}}_{\text{exc}} \exp[i\mathbf{k}_{+}^s \cdot \mathbf{r}] \left(\frac{2i \sin(\rho \sin \theta L)}{i\rho \sin \theta} \right) \\ &\times \left(\frac{\exp[i(k_y^i - \sqrt{k_m^2 - \rho^2})(y_j - 2a)] - \exp[-i(k_y^i - \sqrt{k_m^2 - \rho^2})L]}{i(k_y^i - \sqrt{k_m^2 - \rho^2})} \right). \end{aligned} \quad (\text{A5})$$

We can readily compare both fields. The difference in magnitude of the integrals comes mainly from the effect of the “sinc” function $\sin[(\gamma - \rho \sin \theta)\chi]/(\gamma - \rho \sin \theta)$ in the corresponding integrands, where γ and χ are $\gamma = k_y^i$ and $\chi = 2a$ in Eq. (A4) and, $\gamma = 0$ and $\chi = L$ in Eq. (A5). As is well known, the integral of $\sin[\chi u]/u$ over du from 0 to ∞ is $\pi/2$ regardless of the value of χ . In the second case, Eq. (A5), we see that in the limit $L \rightarrow \infty$, the sinc function behaves as a delta function (since $\chi \rightarrow \infty$), resulting in a definite contribution upon realizing the integral over ρ , whereas in the first case, Eq. (A4), the sinc function spreads over a large interval on ρ and oscillates taking positive and negative values (since now χ is fixed at $2a$). Being the rest of the integrand also an oscillatory function of ρ , we have that the integral over ρ in Eq. (A4) does not accumulate a relevant contribution compared to that in Eq. (A3). Therefore, we conclude that in the limit $L \rightarrow \infty$ we have $\mathbf{E}_{\text{LSS}}^{\text{ind}}(\mathbf{r}) \ll \mathbf{E}_B^{\text{ind}}(\mathbf{r})$. Similarly, we also conclude $\mathbf{E}_{\text{RSS}}^{\text{ind}}(\mathbf{r}) \ll \mathbf{E}_B^{\text{ind}}(\mathbf{r})$.

APPENDIX B

Let us consider Eq. (27) in the text above. The integration variable is k_z^s while k_y^s is a function of k_z^s . We find it convenient to do a change of variable and assume k_y^s as the integration variable. Then, k_z^s becomes a function of k_y^s . For clarity we write the new variable as u . Thus, we have $u = [k_m^2 - (k_z^s)^2]^{1/2}$ and thus, $k_z^s = [k_m^2 - u^2]^{1/2}$. Rewriting Eq. (27) as an integral over u gives

$$\mathbf{E}_B^{\text{ind}}(\mathbf{r}, \mathbf{r}_j) = -\frac{i\rho_s}{4\pi} E_{\text{exc}} \int_{\Gamma} \frac{du}{\sqrt{k_m^2 - u^2}} \left(\frac{i4\pi}{k_m} \right) \mathbf{S}(\mathbf{k}_+^s, \mathbf{k}^{\text{exc}}) \exp[i\mathbf{k}_+^s \cdot \mathbf{r}] \times \frac{\exp[i(k_y^i - u)(y_j - 2a)] - \exp[-i(k_y^i - u)L]}{i(k_y^i - u)}, \quad (\text{B1})$$

where we used $dk_z^s = -udu/[k_m^2 - u^2]^{1/2}$ and $\mathbf{S}(\mathbf{k}_+^s, \mathbf{k}^{\text{exc}})$ is defined by Eq. (29). Recall that here, $\mathbf{k}_+^s = +k_y^s \hat{\mathbf{a}}_y + k_z^s \hat{\mathbf{a}}_z$ with $k_y^s = [k_m^2 - (k_z^s)^2]^{1/2}$ and we are assuming $y > y_j - a$. Then we must have $\text{Im}(k_y^i) > 0$ at all times.

Let us identify the path of integration Γ in the variable u bearing in mind that the integral over dk_z^s goes from $-\infty$ to $+\infty$. Note that u (i.e., k_y^s) has a positive real and a positive imaginary part at all times (this is a requirement from the dyadic Green's function expansion). Then the path of integration in the variable u is the following: u varies from $i\infty$ to zero along the imaginary axis while taking the real part of $k_z^s = \pm[k_m^2 - u^2]^{1/2}$ negative (which varies from $-\infty$ to $-k_m$). Then u goes from 0 to $+k_m$ (along the real axis) and k_z^s varies from $-k_m$ to zero. This path is shown in Fig. 11(a) by the dashed lines. Then, u goes back to zero along the real axis, and finally it goes up the imaginary axis towards $i\infty$, but now we must choose the real part of k_z^s as positive (which goes from zero to $+k_m$ and then from $+k_m$ to ∞). This path is shown in Fig. 11(b).

Thus the integral in Eq. (B1) can be split in two. One along the path Γ_1 in Fig. 11(a) where we must choose $\text{Re}(k_z^s) < 0$ and another along the path Γ_2 in Fig. 11(b) where we must choose $\text{Re}(k_z^s) > 0$. In both cases we must choose the imaginary part with the opposite sign. Then we can write

$$\mathbf{E}_B^{\text{ind}}(\mathbf{r}, \mathbf{r}_j) = \frac{\rho_s}{k_m} E_{\text{exc}} \int_{\Gamma_1} \mathbf{f}(u; \text{Re}(k_z^s) < 0) du + \frac{\rho_s}{k_m} E_{\text{exc}} \int_{\Gamma_2} \mathbf{f}(u; \text{Re}(k_z^s) > 0) du,$$

where

$$\mathbf{f}(u) = \frac{\exp[i\mathbf{k}_+^s \cdot \mathbf{r}]}{\sqrt{k_m^2 - u^2}} \mathbf{S}(\mathbf{k}_+^s, \mathbf{k}^{\text{exc}}) \times \frac{\exp[i(k_y^i - u)(y_j - 2a)] - \exp[-i(k_y^i - u)L]}{i(k_y^i - u)}.$$

Note that each integral consists of the contribution of two segments, either C_1 and C_2 or $-C_1$ and $-C_2$ (see the figures). So we can write the first integral along Γ_1 [Fig. 11(a)] as $\mathbf{E}_{C_1} + \mathbf{E}_{C_2}$ and the other one along Γ_1 [Fig. 11(b)] as $\mathbf{E}_{-C_1} + \mathbf{E}_{-C_2}$ where each term is the contribution to the induced electric field by the integral along the corresponding segment.

Note that, for a large but finite value of L , there is a removable singularity in \mathbf{f} at $u = k_y^i$. (Both, the numerator and denominator, become zero at this point but the quotient remains finite.) Then the integrals over segments C_2 and $-C_2$ are equal to their principal value defined by removing an infinitely small segment around $u = k_y^i$. Therefore, we have

$$\mathbf{E}_B^{\text{ind}}(\mathbf{r}, \mathbf{r}_j) = \frac{\rho_s}{k_m} E_{\text{exc}} \left[\text{P} \int_{\Gamma_1} \mathbf{f}(u; \text{Re}(k_z^s) < 0) du + \text{P} \int_{\Gamma_2} \mathbf{f}(u; \text{Re}(k_z^s) > 0) du \right], \quad (\text{B2})$$

where P means taking the principal value.

Now let us consider the limit $L \rightarrow \infty$. We can remove the term $\exp[-i(k_y^i - u)L]$ from the function $\mathbf{f}(u)$ since it oscillates infinitely fast (except on an infinitesimally small segment around $u = k_y^i$ which is removed by taking the principal value). Upon doing so we introduce a singularity at $u = k_y^i$ but it does not modify the result since we need only the principal value of the integral. Let us denote the resulting function as $\mathbf{f}_{\text{sing}}(u)$.

Now, to evaluate, at least approximately, the principal value of the remaining integrals we make use of Cauchy's theorem. Let us close the contours of integration used in Eq. (B2). To the first integral in Eq. (B1) let us add a semicircle (C_5) of radius $\varepsilon_s \rightarrow 0$ above the singularity and the segments C_3 , C_4 shown in Fig. 12(a). To the second integral we add the same segments, but since these are traveled in the opposite direction we will denote them as $-C_3$, $-C_4$, and $-C_5$ as shown in Fig. 12(b). The integrals over both closed contours are zero since no poles are enclosed and the branch cuts of the function $k_z^s = [k_m^2 - u^2]^{1/2}$ can be taken such that they do not cross the enclosed area. The contribution of the segments C_5 and $-C_5$ can be calculated by standard methods and give $-i\pi[(k_y^i - u)\mathbf{f}_{\text{sing}}(u; \text{Re}(k_z^s) < 0)]_{u=k_y^i}$ and $+i\pi[(k_y^i - u)\mathbf{f}_{\text{sing}}(u; \text{Re}(k_z^s) > 0)]_{u=k_y^i}$ for the integration paths with Γ_1 and Γ_2 , respectively.

Note that within the enclosed area the imaginary part of the number we are taking the square root in $k_z^s = [k_m^2 - u^2]^{1/2}$ is negative, thus we must take the imaginary part of this square root with the opposite sign of that of the real part. That is, we take $\text{Im}(k_z^s) > 0$ when $\text{Re}(k_z^s) < 0$ and $\text{Im}(k_z^s) < 0$ when

$\text{Re}(k_z^s) > 0$. It is not difficult to see that the integrand, $\mathbf{f}_{\text{sing}}(u)$, decays exponentially as $|u| \rightarrow \infty$ within the enclosed area, whether z is positive or negative. In fact, we have that the product, $\exp[iu(y - y_j + b)] \exp[ik_z^s z]$ decays exponentially as $\text{Im}(u)$ increases to infinity. In particular, we must note that in the limit $u_i \rightarrow \infty$, while keeping u_r finite (as in the enclosed area), we have that $\text{Im}(k_z^s)$ remains finite. To prove this, note that $k_z^s = \sqrt{a + ib}$ with $a = k_m^2 - u_r^2 + u_i^2$ and $b = -2u_r u_i$. In the limit $u_i \rightarrow \infty$, while keeping u_r finite (as in the enclosed area) we have that $a \rightarrow u_i^2$ and we have

$$\begin{aligned} \text{Im}(k_z^s) &\rightarrow \pm \sqrt{\frac{-u_i^2 + \sqrt{u_i^4 - 4u_r^2 u_i^2}}{2}} \\ &= \pm \sqrt{\frac{-u_i^2 + u_i^2 \sqrt{1 - 4u_r^2/u_i^2}}{2}} \\ &\rightarrow \pm \sqrt{\frac{-u_i^2 + u_i^2(1 - 2u_r^2/u_i^2)}{2}} \rightarrow \pm u_r, \end{aligned}$$

where $u_i \equiv \text{Im}(u)$ and $u_r \equiv \text{Re}(u)$. Therefore, $\text{Im}(k_z^s)$ remains finite, and so does the factor $\exp[ik_z^s z]$ for $|z| < a$. Conversely, the factor $\exp[iu(y - y_j + b)]$ decays exponentially as u_i increases, since $y - y_j + b$ is assumed positive. Therefore we see that the contributions from C_4 and $-C_4$ are zero.

Now, it is apparent that the contributions from segments C_3 and $-C_3$ are not zero. For instance the contribution from C_3 is given by

$$\begin{aligned} \mathbf{E}_{C_3}(\mathbf{r}, \mathbf{r}_j) &= \frac{\rho_s}{k_m} E_{\text{exc}} \exp[ik_y^i (y_j - 2a)] \\ &\times \int_{C_3} du \frac{\mathbf{S}(\mathbf{k}_+^s, \mathbf{k}^{\text{exc}}) \exp[iu(y - y_j + 2a)]}{\sqrt{k_m^2 - u^2} i(k_y^i - u)} \\ &\times \exp[i\sqrt{k_m^2 - u^2} z], \end{aligned} \quad (\text{B3})$$

where we take the real part of $(k_m^2 - u^2)^{1/2}$ negative and its imaginary part positive. For \mathbf{E}_{-C_3} we get the same integral except for a negative sign (the integral is performed in the opposite direction) and we must take the real part of the square root $(k_m^2 - u^2)^{1/2}$ positive and its imaginary part negative. Note that, along the paths of integration C_3 and $-C_3$ we can do $u = k_m + i\varepsilon$ and integrate on $du = i\varepsilon d\varepsilon$. It then becomes clear that these contributions consist of the integrals of only evanescent fields of the form $\exp[i(k_m + i\varepsilon)y] \exp\{i[k_m^2 - (k_m + i\varepsilon)^2]^{1/2} z\}$. (Recall that an evanescent field is a plane wave with a complex wave vector with its real and imaginary parts orthogonal to each other.)

Then we have

$$\begin{aligned} \mathbf{E}_{C_1} + \mathbf{E}_{C_2} - i\pi \frac{\rho_s}{k_m} E_{\text{exc}} [(k_y^i - u) \mathbf{f}_{\text{sing}}(u; \text{Re}(k_z^s) < 0)]_{u=k_y^i} \\ + \mathbf{E}_{C_3} = 0, \end{aligned} \quad (\text{B4})$$

$$\begin{aligned} \mathbf{E}_{-C_1} + \mathbf{E}_{-C_2} + i\pi \frac{\rho_s}{k_m} E_{\text{exc}} [(k_y^i - u) \mathbf{f}_{\text{sing}}(u; \text{Re}(k_z^s) > 0)]_{u=k_y^i} \\ + \mathbf{E}_{-C_3} = 0. \end{aligned} \quad (\text{B5})$$

Finally, we obtain $\mathbf{E}_B^{\text{ind}}(\mathbf{r}, \mathbf{r}_j)$ as,

$$\begin{aligned} \mathbf{E}_B^{\text{ind}}(\mathbf{r}, \mathbf{r}_j) &= -\frac{\pi \rho_s}{k_z^i k_m} E_{\text{exc}} (\mathbf{S}(\mathbf{k}^i, \mathbf{k}^{\text{exc}}) \exp[i\mathbf{k}^i \cdot \mathbf{r}] \\ &+ \mathbf{S}(\mathbf{k}^r, \mathbf{k}^{\text{exc}}) \exp[i\mathbf{k}^r \cdot \mathbf{r}]) - \rho_s \eta_L^{C_3}(\mathbf{r}, \mathbf{r}_j) \\ &- \rho_s \eta_L^{-C_3}(\mathbf{r}, \mathbf{r}_j), \end{aligned} \quad (\text{B6})$$

where $\eta_B^{C_3}(\mathbf{r}, \mathbf{r}_j) \equiv \mathbf{E}_{C_3}(\mathbf{r}, \mathbf{r}_j)/\rho_s$ are readily obtained from Eq. (B3) and is proportional to the integrals of only evanescent fields. Similarly we find an expression for $\eta_B^{-C_3}(\mathbf{r}, \mathbf{r}_j) \equiv \mathbf{E}_{-C_3}(\mathbf{r}, \mathbf{r}_j)/\rho_s$ in terms of the integral of only evanescent waves.

Now, the contribution from the induced fields from the top half-plane is

$$\begin{aligned} \mathbf{E}_T^{\text{ind}}(\mathbf{r}, \mathbf{r}_j) &= \frac{i\rho_s}{2} E_{\text{exc}} \int \frac{dk_z^s}{2\pi} \frac{\mathbf{S}(\mathbf{k}_-^s, \mathbf{k}^{\text{exc}})}{k_y^s} \\ &\times \frac{\exp[i(k_y^i + k_y^s)L] - \exp[i(k_y^i + k_y^s)(y_j + 2a)]}{i(k_y^i + k_y^s)} \\ &\times \exp[i\mathbf{k}_-^s \cdot \mathbf{r}]. \end{aligned} \quad (\text{B7})$$

This integral can be treated in the same way described above. Again, we take k_y^s as the variable of integration and denote it as u . The integral is split in two, one integral along the path Γ_1 and the other along Γ_2 shown in Fig. 11. In the first case we take $\text{Re}(k_z^s) < 0$ whereas in the second as we take $\text{Re}(k_z^s) > 0$. Then, we close the corresponding contours with either C_3 and C_4 or $-C_3$ and $-C_4$ as we did before. The difference here is that when we drop the rapidly oscillating term (with L the in the argument) we do not introduce a singularity. Then, in this case we get

$$\begin{aligned} \mathbf{E}_T^{\text{ind}}(\mathbf{r}, \mathbf{r}_j) &= \mathbf{E}_{C_1} + \mathbf{E}_{C_2} + \mathbf{E}_{-C_1} + \mathbf{E}_{-C_2} \\ &= -\mathbf{E}_{C_3} - \mathbf{E}_{-C_3} \equiv -\rho_s \eta_T^{C_3} - \rho_s \eta_T^{-C_3}, \end{aligned}$$

where

$$\begin{aligned} \eta_T^{C_3}(\mathbf{r}, \mathbf{r}_j) &= \frac{1}{k_m} E_{\text{exc}} \exp[ik_y^i (y_j + 2a)] \\ &\times \int_0^\infty d\varepsilon \frac{\mathbf{S}(\mathbf{k}_-^s, \mathbf{k}^{\text{exc}})}{\sqrt{k_m^2 - (k_m + i\varepsilon)^2}} \\ &\times \frac{\exp[-i(k_m + i\varepsilon)(y - y_j - 2a)]}{(k_y^i + k_m + i\varepsilon)} \\ &\times \exp(i\sqrt{k_m^2 - (k_m + i\varepsilon)^2} z) \end{aligned} \quad (\text{B8})$$

with $\mathbf{k}_-^s = -(k_m + i\varepsilon)\hat{\mathbf{a}}_y + [k_m^2 - (k_m + i\varepsilon)^2]^{1/2}\hat{\mathbf{a}}_z$ and we should take the real part of $[k_m^2 - (k_m + i\varepsilon)^2]^{1/2}$ negative and its imaginary part positive. A similar result is found for $\eta_T^{-C_3}(\rightarrow r)$ but the integral goes from $\varepsilon = \infty$ to zero and we take the real and imaginary parts of $[k_m^2 - (k_m + i\varepsilon)^2]^{1/2}$ positive and negative, respectively.

APPENDIX C

Introducing the exciting field given in Eq. (33) into Eq. (10), using the plane wave expansion to the dyadic Green's function given in (39) and the momentum representation of the transition operator in Eq. (4) yields

$$\begin{aligned}
\mathbf{E}(\mathbf{r}) = & \mathbf{E}^i(\mathbf{r}) + \frac{i\rho}{2} \int d^3r' \iint \frac{dk_x^s dk_y^s}{(2\pi)^2} \frac{1}{k_z^s} (\hat{\mathbf{I}} - \hat{\mathbf{k}}_{\pm}^s \hat{\mathbf{k}}_{\pm}^s) \\
& \cdot \exp[i\mathbf{k}_{\pm}^s \cdot (\mathbf{r} - \mathbf{r}')] \int d^3r'' \int \frac{d^3p'}{(2\pi)^3} \int \frac{d^3p''}{(2\pi)^3} \\
& \times \int_V d^3r_n \exp(ip' \cdot [\mathbf{r}' - \mathbf{r}_n]) \mathbf{T}(\mathbf{p}', \mathbf{p}'') \\
& \cdot \exp(-ip'' \cdot [\mathbf{r}'' - \mathbf{r}_n]) [E_1 \exp(i\mathbf{k}^i \cdot \mathbf{r}'') \hat{\mathbf{e}}_i \\
& + E_2 \exp(i\mathbf{k}^r \cdot \mathbf{r}'') \hat{\mathbf{e}}_r], \tag{C1}
\end{aligned}$$

valid for $|z| > a$. The integration region over $d^3r_n = dx_n dy_n dz_n$ is a $L \times L \times \Delta z$ volume where we will take the limits $L \rightarrow \infty$ and $\Delta z \rightarrow 0$ after performing the integrals. Again the integrals over d^3r' and d^3r'' can be done readily and give the factors $(2\pi)^3 \delta(\mathbf{p}'' - \mathbf{k}^i)$ and $(2\pi)^3 \delta(\mathbf{p}' - \mathbf{k}_{\pm}^s)$. Then, the integrals over d^3p' and d^3p'' are trivial. We get

$$\begin{aligned}
\mathbf{E}(\mathbf{r}) = & \mathbf{E}^i(\mathbf{r}) + \frac{i\rho}{2} \iint \frac{dk_x^s dk_y^s}{(2\pi)^2} \frac{1}{k_z^s} (\hat{\mathbf{I}} - \hat{\mathbf{k}}_{\pm}^s \hat{\mathbf{k}}_{\pm}^s) \cdot \exp[i\mathbf{k}_{\pm}^s \cdot \mathbf{r}] \\
& \times \int_V d^3r_n [E_1 \exp[i(\mathbf{k}^i - \mathbf{k}_{\pm}^s) \cdot \mathbf{r}_n] \hat{\mathbf{T}}(\mathbf{k}_{\pm}^s, \mathbf{k}^i) \\
& \cdot \exp(i\mathbf{k}^i \cdot \mathbf{r}_n) \hat{\mathbf{e}}_i + E_2 \exp[i(\mathbf{k}^r - \mathbf{k}_{\pm}^s) \cdot \mathbf{r}_n] \hat{\mathbf{T}}(\mathbf{k}_{\pm}^s, \mathbf{k}^r) \cdot \hat{\mathbf{e}}_r \\
& \times \exp(i\mathbf{k}^r \cdot \mathbf{r}_n)]. \tag{C2}
\end{aligned}$$

The integrals over dx_n and dy_n go from $-L$ to L with $L \rightarrow \infty$ and give the factors, $2\pi\delta(k_x^s)$ and $2\pi\delta(k_y^s - k_y^i)$ respectively (recall that $k_x^i = 0$). The integral over dz_n goes from 0 to Δz and gives the factor $\Delta z \rightarrow 0$. Using the definition in Eq. (29), $\mathbf{S}(\mathbf{q}, \mathbf{p}) \equiv (k_m/i4\pi)(\hat{\mathbf{I}} - \hat{\mathbf{q}}\hat{\mathbf{q}}) \cdot \mathbf{T}(\mathbf{q}, \mathbf{p}) \cdot \hat{\mathbf{e}}_p$ we get for $|z| > a$,

$$\begin{aligned}
\mathbf{E}(\mathbf{r}) = & \mathbf{E}^i(\mathbf{r}) - \alpha E_1 \mathbf{S}(\mathbf{k}_{\pm}^s, \mathbf{k}^i) \exp[i\mathbf{k}_{\pm}^s \cdot \mathbf{r}] \\
& - \alpha E_2 \mathbf{S}(\mathbf{k}_{\pm}^s, \mathbf{k}^r) \exp[i\mathbf{k}_{\pm}^s \cdot \mathbf{r}], \tag{C3}
\end{aligned}$$

where $\mathbf{k}_{\pm}^s = k_y^i \hat{\mathbf{a}}_y \pm k_z^i \hat{\mathbf{a}}_z$ with $k_y^i = k_m \sin \theta_i$ and $k_z^i = k_m \cos \theta_i$ and the “+” sign is for $z > 0$ whereas the “-” one is for $z < 0$.

ACKNOWLEDGMENTS

We acknowledge financial support from Consejo Nacional de Ciencia y Tecnología (México) through grants 49482F and 82073 and from Dirección General de Asuntos del Personal Académico of the Universidad Nacional Autónoma de México through grants IN-120309 and IN-111710.

†On sabbatical leave from Centro de Ciencias Aplicadas y Desarrollo Tecnológico, Universidad Nacional Autónoma de México, Apartado Postal 70-186, Distrito Federal 04510, Mexico.

REFERENCES

1. T. Okamoto, I. Yamaguchi, and T. Kobayashi, “Local plasmon sensor gold colloid monolayers deposited upon glass substrates,” *Opt. Lett.* **25**, 372–374 (2000).
2. G. Xu, Y. Chen, M. Tazawa, and P. Jin, “Influence of dielectric properties of a substrate upon plasmon resonance spectrum supported Ag nanoparticles,” *Appl. Phys. Lett.* **88**, 043114 (2006).
3. C. Kuemin, T. Kraus, H. Wolf, and N. D. Spencer, “Matrix effects on the surface plasmon resonance of dry supported gold nanocrystals,” *Opt. Lett.* **33**, 806–808 (2008).
4. D.-S. Wang and C.-W. Lin, “Density-dependent optical response of gold nanoparticle monolayers on silicon substrates,” *Opt. Lett.* **32**, 2128–2130 (2007).
5. T. Yamaguchi, H. Takahashi, and A. Sudoh, “Optical behavior of a metal island film,” *J. Opt. Soc. Am.* **68**, 1039–1044 (1978).
6. A. Bagchi, R. G. Barrera, and A. K. Rajagopal, “Perturbative approach to the calculation of the electric field near a metal surface,” *Phys. Rev. B* **20**, 4824–4838 (1979).
7. A. Bagchi, R. G. Barrera, and R. Fuchs, “Local-field effect in optical reflectance from adsorbed overlayers,” *Phys. Rev. B* **25**, 7086–7096 (1982).
8. V.-V. Truong, G. Bosi, and T. Yamaguchi, “Optical behaviour of granular metal films: single-image versus multiple-image approaches in the treatment of substrate effects,” *J. Opt. Soc. Am. A* **5**, 1379–1381 (1988).
9. R. G. Barrera, M. del Castillo-Mussot, G. Monsivais, P. Villaseñor, and W. L. Mochán, “Optical properties of two-dimensional disordered systems on a substrate,” *Phys. Rev. B* **43**, 13819–13826 (1991).
10. G. Bosi, “Transmission of a thin film of spherical particles on a dielectric substrate: the concept of effective medium revisited,” *J. Opt. Soc. Am. B* **9**, 208–213 (1992).
11. G. Bosi, “Optical response of a thin film of spherical particles on a dielectric substrate: retarded multipolar treatment,” *J. Opt. Soc. Am. B* **11**, 1073–1083 (1994).
12. G. Bosi, “Optical response of a thin film of spherical particles upon a dielectric substrate: retarded multipolar treatment including multiple reflections,” *J. Opt. Soc. Am. B* **13**, 1691–1696 (1996).
13. V. A. Fedotov, V. I. Emel'yanov, K. F. MacDonald, and N. I. Zheludev, “Optical properties of closely packed nanoparticle films: spheroids and nanoshells,” *J. Opt. Pure Appl. Opt.* **6**, 155–160 (2004).
14. J. Toudert, D. Babonneau, L. Simonot, S. Camelio, and T. Girardeau, “Quantitative modelling of the surface plasmon resonances of metal nanoclusters sandwiched between dielectric layers: the influence of nanocluster size, shape and organization,” *Nanotechnology* **19**, 125709 (2008).
15. M. L. Protopapa, A. Rizzo, M. Re, and L. Piloni, “Layered silver nanoparticles embedded in a BaF₂ matrix: optical characterization,” *Appl. Opt.* **48**, 6662–6669 (2009).
16. M. L. Protopapa, “Surface plasmon resonance of metal nanoparticles sandwiched between dielectric layers: theoretical modeling,” *Appl. Opt.* **48**, 778–785 (2009).
17. T. Menegotto, M. B. Pereira, R. R. B. Correia, and F. Horowitz, “Simple modeling of plasmon resonances in Ag/SiO₂ nanocomposite monolayers,” *Appl. Opt.* **50**, C27–C30 (2011).
18. R. G. Barrera and A. García-Valenzuela, “Coherent reflectance in a system of random Mie scatterers and its relation to the effective medium approach,” *Opt. J. Soc. Am. A* **20**, 296–311 (2003).
19. A. García-Valenzuela and R. G. Barrera, “Electromagnetic response of a random half-space of Mie scatterers within the effective field approximation and the determination of the effective optical coefficients,” *J. Quant. Spectrosc. Radiat. Transfer* **79-80**, 627–647 (2003).
20. R. G. Barrera, A. Reyes-Coronado, and A. García-Valenzuela, “Nonlocal nature of the electrodynamic response of colloidal systems,” *Phys. Rev. B* **75**, 184202 (2007).
21. L. Tsang and J. A. Kong, *Scattering of Electromagnetic Waves; Advanced Topics* (Wiley, 2001).
22. E. A. van der Zeeuw, L. M. Sagis, G. J. M. Koper, Mann, M. T. Haarmans, and D. Bedeaux, “The suitability of angle scanning reflectometry for colloidal particle sizing,” *J. Chem. Phys.* **105**, 1646–1653 (1996).
23. K. M. Hong, “Multiple scattering of electromagnetic waves by a crowded monolayer of spheres: Application to migration imaging films,” *J. Opt. Soc. Am.* **70**, 821–826 (1980).
24. K. M. Hong, “Granularity of monolayers: hard-disk model,” *J. Opt. Soc. Am. A* **5**, 237–240 (1988).
25. V. P. Dick, V. A. Loiko, and A. P. Ivanov, “Angular structure of radiation scattered by monolayers of particles: experimental study,” *Appl. Opt.* **36**, 4235–4240 (1997).
26. V. A. Loiko, V. P. Dick, and V. I. Molochko, “Monolayers of discrete scatterers: comparison of the single-scattering and

- quasi-crystalline approximations,” *J. Opt. Soc. Am. A* **15**, 2351–2354 (1998).
27. V. A. Loiko, V. P. Dick, and A. P. Ivanov, “Features in coherent transmittance of a monolayer of particles,” *J. Opt. Soc. Am. A* **17**, 2040–2045 (2000).
 28. V. A. Loiko and A. A. Miskevich, “Light propagation through a monolayer of discrete scatterers: analysis of coherent transmission and reflection coefficients,” *Appl. Opt.* **44**, 3759–3768 (2005).
 29. M. C. Peña-Gomar, J. J. F. Castillo, A. García-Valenzuela, R. G. Barrera, and E. Pérez, “Coherent optical reflectance from a monolayer of large particles adsorbed on a glass surface,” *Appl. Opt.* **45**, 626–632 (2006).
 30. A. Ponyavina, S. Kachan, and N. Sil’vanovich, “Statistical theory of multiple scattering of waves applied to three-dimensional layered photonic crystals,” *J. Opt. Soc. Am.* **21**, 1866–1875 (2004).
 31. J. J. H. Wang, “A unified and consistent view on the singularities of the electric dyadic Green’s function in the source region,” *IEEE Trans. Antennas Propag.* **30**, 463–468 (1982).
 32. M. I. Mishchenko, “Multiple scattering by particles embedded in an absorbing medium. 1. Foldy-Lax equations, order-of-scattering expansion, and coherent field,” *Opt. Express* **16**, 2288–2301 (2008).
 33. R. G. Barrera and C. I. Mendoza, “Three-particle correlations in the optical properties of granular composites,” *Solar Energy Mater. Solar Cells* **32**, 463–476 (1994).
 34. J. K. Percus and G. J. Yevick, “Analysis of classical statistical mechanics by means of collective coordinates,” *Phys. Rev.* **110**, 1–13 (1958).
 35. S. Durant, O. Calvo-Perez, N. Vukadinovic, and J. J. Greffet, “Light scattering by a random distribution of particles in an absorbing media: full-wave Monte Carlo Solutions of the extinction coefficient,” *J. Opt. Soc. Am. A* **24**, 2953–2961 (2007).
 36. W. C. Chew, *Waves and Fields in Inhomogeneous Media*, IEEE Press Series on Electromagnetic Waves (IEEE, 1995), Chap. 7.
 37. C. F. Bohren and D. R. Huffman, *Absorption and Scattering of Light by Small Particles*, (Wiley-Interscience, 1983).